Scaling Limits of Interacting Particle Systems: The Case of SOS and WASEP

Johanna Heideman

Master's thesis
2023:E77

Lund University

Faculty of Engineering
Centre for Mathematical Sciences
Mathematics

Centrum Scientiarum Mathematicarum

Abstract

The aim of this thesis is to provide a comprehensive introduction to interacting particle systems and their scaling limits by investigating two particle systems: the Solid On Solid growth process (SOS) and the Weakly Asymmetric Simple Exclusion Process (WASEP).
An interacting particle system is a stochastic process describing the evolution of finitely or infinitely many particles, each of which, in the absence of any interaction, would evolve like a Markov process. The particle system can be examined in different scales by grouping particles together and considering their average. Their behaviour is described by a Markov process on a microscopic scale, while on a macroscopic scale, it is represented by a partial differential equation. In the scaling limit, both the deterministic and stochastic properties are significant, and a stochastic differential equation characterizes the particle system.
The WASEP and SOS are, though modelling different physical phenomena, related in that the WASEP can be seen as the discrete derivative of the SOS. It was thus sufficient to simulate only the WASEP and calculate the value of the SOS after the simulation finished. As expected, the simulations suggest systems with more sites have a smoother final distribution and take longer to converge. When the number of empty and occupied sites in the WASEP was close, the variance was higher, and convergence was faster.
In Bertini and Giacomins paper *Stochastic Burgers and KPZ equations from Particle Systems*, the Kardar-Parisi-Zhang equation was proven to be the hydrodynamic scaling limit to the SOS. Instead of considering the non-linear stochastic PDE directly, they used the Cole-Hopf transform to get the stochastic heat equation, for which the existence and uniqueness of a solution are known. A similar transform, the Gärtner transform, was used on a scaled and linearly interpolated SOS process. The transformed process was shown to converge to the stochastic heat equation, which implies that the SOS converges to the KPZ-equation in the hydrodynamic limit. The same method of proof was used to show the convergence of the WASEP to the stochastic Burgers equation.
The SOS belongs to the KPZ universality class. Models in this class are expected to be invariant under the scaling $h(x,t) = \alpha h(\alpha^{-2}x, \alpha^{-3}t)$. Much of the research on KPZ universality has been done with the SOS since it has the necessary properties to be linearised with the Gärtner transform.

Keywords: Interacting particle systems, Scaling limits, WASEP, SOS, KPZ-equation

Summary

The Weakly Asymmetric Simple Exclusion Process (WASEP) is a model used to, for example, describe the internal movement of a collection of gas molecules with the assumption that space is divided into discrete spaces. These spaces have room for one molecule and can be either occupied or empty. Here, the WASEP is modelled in one dimension. After a random amount of time, a molecule will attempt to move one step to the left or one step to the right. If the neighbouring spot is empty, it will succeed. Regardless of whether it moved or not, it will again wait for a random time to move. Weakly Asymmetric means that the particles are slightly more likely to want to move left than right. No matter where the particles were initially, after sufficient time, the average concentration of particles at different places on the line will stabilize. How fast this happens depends on how many parts the space is divided into and the proportion of occupied and empty spaces. In a larger system, where space is divided into more spaces, convergence is slower. On the other hand, when there are approximately the same number of occupied and empty spaces, it will converge faster.

The Solid On Solid (SOS) process is a growth process. Among other phenomena, it describes how a crystal forms on a surface. One at a time, particles deposit on, or evaporate from, a place on the border of the crystal and the surrounding material. As deposition occurs slightly more often than evaporation, the crystal will grow. The SOS enforces a single-step constraint on the growth. It means that no molecules at the border are at the same height as their immediate neighbours; they are either one step above or below. As a consequence, deposition is only possible at places where both neighbours are one step higher, i.e. a local minimum. Similarly, the only particles that can evaporate are the ones that are higher than their surroundings.

These two models are related. A molecule moves one step to the left in the WASEP at the same rate as a particle is deposited in the SOS. Further, movement to the left in the WASEP is possible when there is a particle in the original space and none in the left neighbouring space. When this occurs, there is a local minimum in the SOS.

The WASEP and SOS models describe physical phenomena on a microscopic scale, where individual molecules are detectable. When zooming out, only

the average motion is visible. Instead of measuring individual molecules, temperature, volume, and pressure describe the gas. The crystal grows continuously, and the border appears smooth. There is mathematical proof that when appropriately scaling space and time and increasing the number of spaces in the modelled system with time, the particle system models will converge to stochastic differential equations.

Acknowledgements

I would like to express my gratitude to my supervisors, Dr Carina Geldhauser and Dr Filip Bar, for their guidance and support. I would also like to thank my family for their encouragement.

Contents

Chapter 1

Introduction: scaling limits of particle systems

Statistical mechanics is a branch of physics with the goal of connecting the observed macroscopic features of a physical system with the properties of their microscopic constituents. The study of interacting particle systems originated from statistical mechanics with the aim to better understand phenomena such as phase transition. Since then, models with similar mathematical structures have been formulated to describe various physical phenomena. Among these are ferromagnetism under an external magnetic field, the spread of infection, tumour growth and the process in which two species switch territories.

Mathematically, an interacting particle system is a stochastic process describing the evolution of finitely or infinitely many particles, each of which, in the absence of any interaction, would evolve like a Markov process. Like the physical systems they model, their properties depend on the scale. On a local level, their movement is random. Going to a coarser scale is done by grouping particles together and considering their average values. Eventually, the scale grows coarser, and the evolution of the system will become independent of the stochastic fluctuations from the Markov processes. Instead, a partial differential equation describes the evolution.

Assume the realisation of a particle system is on a finite interval which contains N discrete points that are the possible positions for a particle. These positions are called sites. As $N \to \infty$, the distance between particles will go

to 0. Instead of a Markov process, a partial differential equation will describe the evolution of the system. The correct scaling in time and space is needed to see both the deterministic evolution and the random fluctuations of the system. In this scaling, there will be an equilibrium state (Lan02). On this level, the evolution of the system depends on both random noise and a partial differential equation and is described with a stochastic partial differential equation. Using a diffusive scaling , $t \sim \varepsilon^{-2}t$, $x \sim \varepsilon^{-1}x$, the equation found as $N \to \infty$ is called the hydrodynamic scaling limit.

The Kardar-Parisi-Zhang (KPZ) equation appears in the scaling limit for many particle systems and other models. It is an ill-posed non-linear stochastic partial differential equation. In 1997, Bertini and Giacomin (Ber97) successfully solved it by linearisation and showed that it converged to the same function as was found in the scaling limit of the (Weakly Asymmetric) Single Step Solid on Solid process.

The Single Step Solid on Solid Process is a growth process and one of the two processes examined here. The other is the Weakly Asymmetric Simple Exclusion Process that models particles on a shifting place on a lattice. Though modelling different kinds of physical systems, the two processes are related in the sense that the latter can be interpreted as the discrete derivative of the former.

This thesis aims to introduce particle systems and scaling limits and provide a comprehensive overview of the ideas presented in (Ber97). The focus will be on the two particle systems described in (Ber97), and their behaviour at a microscopic level and in the limit is investigated theoretically and with simulations.

Chapter 2 presents the mathematics used for studying particle systems and their scaling limits. It includes a brief discussion of Markov processes in Section 2.1, stochastic calculus with a focus on interpreting a stochastic partial differential equation in Section 2.2 and what it means for a stochastic process to converge in Section 2.3. Some definitions from probability theory can be found in the Appendix A. These include σ-fields, filtrations, random variables, and stochastic processes.

Chapter 3 describes the two studied particle systems. Exclusion processes,

exemplified by the Weakly Asymmetric Simple Exclusion Process (WASEP), are introduced in Section 3.1. This Section also covers the tagged particle process. Section 3.2 presents the Weakly Asymmetric Single Step Solid On Solid Process (SOS), and Section 3.3 contains a description of the relationship between the processes.

Chapter 4 contains simulations of the two particle systems. The method used for simulations is explained in Section 4.1, and the code is found in Appendix B. The results of the simulations are discussed in Sections 4.2 and 4.3. In the former section, a Java animation examines the small-scale behaviour of the particle systems B.2. In the latter, a Matlab simulation explores the long-term behaviour of systems with different sizes and varying numbers of particles B.1.

The theoretical long-term behaviour of the particle systems is analysed in Chapter 5. The derivation of a limiting equation is shown for the symmetric simple exclusion process in Section 5.1, for a gradient exclusion process in Section 5.2 and for the WASEP in Section 5.3. Section 5.4 discusses the limit of the SOS. This Section also introduces the KPZ equation and summarises the relationship between the SOS and the KPZ equation described in the paper by Bertini and Giacomin (Ber97). Finally, Section 5.5 presents the KPZ Universality conjecture.

The last chapter, 6, briefly summarises some of the current research on particle systems and KPZ universality.

Chapter 2

Mathematical background

The dynamics of a particle system differ depending on scale. At the microscopic scale, the random movement of individual particles dominates, and the system is characterised by a stochastic process. In the macroscopic scale, where individual particles are no longer discernible, a partial differential equation is used to describe the average dynamics of the particles. When rescaling from the microscopic scale to the macroscopic, there is a place where both the stochastic process and the differential equation contribute to the observable system dynamics. This is sometimes referred to as the mesoscopic scale. In this scale, the random fluctuations around the average, which cancels out at the macroscopic scale, become significant. The aim of taking a scaling limit is to investigate the behaviour of a particle system at this scale.

Two different models are studied in this thesis; one is an exclusion process, and the other is a growth process. Both these processes are used for modelling several physical phenomena.

Exclusion processes can model, for example, the behaviour of a gas. In this model, space is considered discrete, and only one particle can be in any place. The movement of individual gas molecules and their interaction is studied on a microscopic scale. On the macroscopic scale, the gas is described by thermodynamic state variables, such as temperature and pressure, that depend on the average state of the molecules.

Similarly, if describing the growth of a crystal with a growth process, the microscopic level concerns the deposition and evaporation of individual par-

ticles, and the model on the macroscopic scale is the height of the whole crystal.

Analysis of the particle system models requires different mathematical tools depending on scale. Markov processes model the local particle dynamics. Section 2.1 contains a description of Markov processes and Markov generators.

In the scaling limit, partial differential equations, with an additional dependence on white noise to model the fluctuations around the average, describe the dynamic system. Equations like this are known as stochastic differential equations. Section 2.2 introduces stochastic calculus and stochastic differential equations. Definitions for the concepts used to derive stochastic integrals are found in the Appendix A.

The stochastic partial differential equation that describes the macroscopic behaviour is derived as a limit when the size of the system goes to infinity. Convergence for stochastic processes is discussed in Section 2.3.

2.1 Markov processes

A Markov process is a stochastic process with the property that only the current state of the process determines the next. For a definition of stochastic processes, see Appendix A.3 and for conditional expectations, see Appendix A.2.

Formally, a **Markov process** is defined as a stochastic process ξ_n where

$$\mathrm{P}\big(\xi_{n+1}|\xi_n, \xi_{n-1}, \ldots, \xi_0\big) = \mathrm{P}\big(\xi_{n+1}|\xi_n\big). \tag{2.1}$$

A Markov process is characterised by its intensity matrix $Q = (q_{ij})$ where element q_{ij} is the transition rate from state i to state j. The element q_{ii} is defined to be $q_{ii} = -\sum_{j\neq i} q_{ij}$. As a result, the sum of a row in an intensity matrix will always be 0.

In the absence of interactions with other particles, the movement of a single particle is governed by a Markov process. For a simple exclusion process at a specific time, only the two neighbouring states are reachable for any one

particle. Thus, the only elements which could be positive on row i in the intensity matrix are $q_{i,i+1}$ and $q_{i,i-1}$. Suppose there are N sites in the system. Then, this matrix will be of size $N \times N$. Assume the rate of a jump one step right is λ and the rate one step left is μ. The intensity matrix Q will have $-(\lambda + \mu)$ on the main diagonal, λ on the upper diagonal, μ on the lower diagonal, and 0 at all other positions.

While the intensity matrix for a single particle is possible to write out, such is not the case when the particles are combined into a particle system. The whole particle system is also a Markov process. However, its state space, consisting of all possible configurations of particles, is much larger. A Markov generator is used instead of an intensity matrix to explain its evolution. A Markov generator is a functional acting on $f : \Omega \to \mathbb{R}$. $f(\xi_t)$ is a cylindrical function, which means it has a finite norm and guarantees the statistical properties of the stochastic process ξ_t are unaltered. If the current state of a Markov process such as a particle system is $\xi_t(x)$, the Markov generator L acting on $f(\xi_t)$ is written as a sum over the sites x

$$Lf\big(\xi_t(x)\big) = \sum_x g(\xi_t)\Big[h\Big(f\big(x, \xi_t(x)\big)\Big)\Big], \tag{2.2}$$

where $g(\xi_t)$ is some function describing the transition rates and $\Big[h\Big(f\big(x, \xi_t(x)\big)\Big)\Big]$ describes which sites are possible to transition to from position x. In the case of a single step exclusion process for every x, the possible transitions are to $x + 1$ and $x - 1$, and only for these two positions can $\Big[h\Big(f\big(x, \xi_t(x)\big)\Big)\Big]$ be non-zero.

2.2 Stochastic differential equations

While the large-scale behaviour of a particle system, such as diffusion and drift, can be represented by a deterministic partial differential equation, this model fails to include small random fluctuations from particle movement. A random noise term in the form of some stochastic process can be appended to the equation to rectify this.

The particle systems introduced in Section 3 are studied in $1 + 1$ dimensions. $1 + 1$ refers to one dimension in time and one dimension in space.

How to find a non-trivial scaling limit in more than one space dimension is unclear. The solution to the KPZ equation found in (Ber97) relies on the existence of a solution to the stochastic heat equation, and the solution to the stochastic heat equation is only well defined in one space dimension.

In this Section, stochastic calculus will be introduced for one-dimensional integrals and ordinary differential equations. Consider first the differential equation

$$dX_t = f(X_t)dt + g(X_t)dW_t. \tag{2.3}$$

With a locally Lipschitz continuous function f and appropriate boundary and initial conditions for X_t, the deterministic part $dX_t = f(X_t)dt$ has a unique, well-defined solution. However, with the addition of $g(X_t)dW_t$, a stochastic process proportional to the increments of a Wiener process, it is no longer clear what a solution to equation (2.3) is. A Wiener process is a stochastic process used for modelling uncorrelated noise. It will be defined later in this Section.

As the Wiener process is not differentiable, equation (2.3) lacks rigorous meaning. This is circumvented by extending concepts from calculus to stochastic processes and considering the corresponding integral equation instead of studying the differential equation directly,

$$X(T) = X(0) + \int_0^T f(X_s)ds + \int_0^T g(X_s)dW_s. \tag{2.4}$$

The integral $\int_0^T g(X_s)dW_s$ is an Itô stochastic integral. It integrates over a Wiener process W_t instead of over an interval, which makes it differ from Riemann integrals in calculations, properties and convergence.

The **Wiener process** W_t is a stochastic process with stationary, independent and Normal distributed $\mathcal{N}(0,t)$ increments $W(t) - W(s)$ where $W(0) = 0$ almost surely (a.s.) and the sample paths $t \mapsto W(t)$ are a.s. continuous.(An event A is said to occur **almost surely** if $P(A) = 1$). The Wiener process is a random walk process in one dimension. It is a continuous process, but it is not differentiable. The Wiener process is scale invariant, if W_t is a Wiener process so is $\alpha^{-1}W_{\alpha^2 t}$ for any $\alpha \neq 0$.

Similarly to the Riemann integral, the Itô integral is defined with an approximating sum

$$\int g(t)dW_t = \sum_{j=0}^{n-1} g(s_j)\nabla W_t = \sum_{j=0}^{n-1} g(s_j)\big(W(t_{j+1}) - W(t_j)\big). \tag{2.5}$$

The difference is that the choice of $s_j \in [t_j, t_{j+1}]$ affects the limit of the approximating sum for the stochastic integral. It is advantageous if s_j can be picked so that the approximation at any time t only depends on what is known at t and not on any future events.

For a stochastic process, the concepts of knowledge and time are represented by σ-fields and filtrations, respectively. These are introduced briefly in the Appendix A.1. Filtrations are used in the definitions of random variables and probability spaces. These definitions can be found in the Appendix A.2.

The stochastic function $g(t)$ and the Wiener process W_t in equation (2.5) are both adapted to the filtration $\mathcal{F}_t$. By choosing $s_j = t_j$ in the sum approximating the Itô integral (2.5) will be adapted to the same filtration. Convergence of the sum will be in the space of square integrable random variables.

A function $g(t)$ is called a **random step function** if

$$g(t) = \sum_{j=0}^{n-1} \eta_j 1_{[t_j, t_{j+1}]}(t) \tag{2.6}$$

where $(\eta_j)_{j\in[0,n-1]}$ is a series of square integrable $\mathcal{F}_{t_j}$-measurable random variables. If there is a sequence $g_1(t), g_2(t), \ldots$ such that

$$\lim_{n\to\infty} \mathrm{E}\left(\int_0^\infty \big|g(t) - g_n(t)\big|^2 dt\right) = 0 \tag{2.7}$$

the stochastic function $g(t)$ is said to be approximated by random step functions.

The sum (2.5) converges for functions $g(t)$, which can be approximated by random step functions, are adapted to $\mathcal{F}_t$, have a.s. continuous paths, and

are square integrable. It is for this class of functions the Itô integral exists. Convergence refers to convergence in probability, defined in Section (2.3).

Assume the $\{g_n\}_{n\in\mathbb{N}}$ is a sequence of random step functions converging to a stochastic process g. The **Itô integral** of g is a stochastic process defined by the limit

$$\lim_{n\to\infty} \mathrm{E}\big(|I(g) - I(g_n)|^2\big) = 0 \tag{2.8}$$

where

$$I(f_n) = \sum_{j=0}^{n-1} \eta_j \big(W(t_{j+1}) - W(t_j)\big) \tag{2.9}$$

2.2.1 Computation of the Itô Integral

The non-differentiability of the Wiener process causes an extra term in the computation of the Itô integral compared to the Riemann integral. The Itô formula is written as an Itô process with differential notation. Suppose that $\xi(t)$ is the Itô process satisfying the differential equation

$$d\xi(t) = b(t)dt + \sigma(t)dW_t, \tag{2.10}$$

where $b(t)$ is a stochastic process adapted to the filtration $\mathcal{F}_t$ and is integrable on the interval $[0, T]$ for all $T \geq 0$, and $\sigma(t)$ is an Itô integrable function. Then the **Itô formula** (2.11) satisfies the differential equation (2.10) for $F\big(t, \xi(t)\big)$;

$$\begin{aligned} dF\big(t,\xi(t)\big) = \Big(F'_t\big(t,\xi(t)\big) + F'_x\big(t,\xi(t)\big)b(t) + \frac{1}{2}F''_{xx}\big(t,\xi(t)\big)\sigma^2(t)\Big)dt \\ + F'_x\big(t,\xi(t)\big)\sigma(t)dW_t, \end{aligned} \tag{2.11}$$

and can be used to calculate the value of the stochastic integral.

As an example to illustrate that the Itô formula, equation (2.11), gives the same result as obtained by the definition of the stochastic integral, both are used to compute the stochastic integral $\int_0^T t dW_t$ below.

By the definition: Approximate $F(t) = t$ by a random step function

$$f_n = \sum_{i=0}^{n-1} t_i^n 1_{[t_i^n, t_{i+1}^n]} \tag{2.12}$$

where the interval $[0, T]$ has a partition with n equal parts. The stochastic integral of the step function is

$$I(f_n) = \sum_{i=0}^{n-1} t_i^n \big(W(t_{i+1}^n) - W(t_i^n)\big) \tag{2.13}$$

which is equal to

$$\sum_{i=0}^{n-1} \big(t_{i+1}^n W(t_{i+1}^n) - t_i^n W(t_i^n)\big) - \sum_{i=0}^{n-1} W(t_{i+1}^n)(t_{i+1}^n - t_i^n)$$
$$= TW(T) - \sum_{i=0}^{n-1} W(t_{i+1}^n)(t_{i+1}^n - t_i^n). \tag{2.14}$$

Convergence gives

$$\int_0^T t dW_t = TW(T) - \int_0^t W_t dt. \tag{2.15}$$

Using the Itô formula: To use Itô's formula, consider the integral as a part of an Itô process in differential form

$$d\xi(t) = b(t)dt + t dW_t. \tag{2.16}$$

Comparison with the Itô formula (2.11) finds the dW_t term

$$F_x'(t, x)\sigma(t) = t. \tag{2.17}$$

This is true when $F(x, t) = tx$ and $\sigma(t) = 1$. Aside from F_x' the Itô formula requires the derivatives F_{xx}'' and F_t'. With the choice of $F(x, t) = tx$; $F_{xx}'' = 0$ and $F_t' = x$. Insertion in (2.11) yields

$$dF(t, W_t) = W_t \; dt + t \; dW_t, \tag{2.18}$$

which is a representation of the integral equation

$$TW(T) = \int_0^T W_t dt + \int_0^T t dW_t \tag{2.19}$$

or, equivalently

$$\int_0^T t\ dW_t = TW(T) - \int_0^T W_t\ dt. \tag{2.20}$$

The two methods find the same expression for $\int_0^T t\ dW_t$. The Itô integral has three properties which can be used to find the distribution.

1. *Linearity* Just as the Riemann integral, the Itô integral is linear

$$\int_0^t \big(\alpha f(r) + \beta g(r)\big)dW_r = \alpha \int_0^t f(r)dW_r + \beta \int_0^t g(r)dW_r \tag{2.21}$$

2. *Isometry* There is an isometry between the Itô and the Riemann integral

$$\mathrm{E}\left(\Big|\int_0^t f(r)dW_r\Big|^2\right) = \mathrm{E}\left(\int_0^t |f(r)|^2 dr\right) \tag{2.22}$$

3. *Martingale property* The expectation of its value at any time in the future is equal to the current value

$$\mathrm{E}\left(\int_0^t f(r)dW_r|\mathcal{F}_s\right) = \int_0^s f(r)dW_r \tag{2.23}$$

Finding the distribution of $\int_0^T t\ dW_t = TW(T) - \int_0^T W_t\ dt$: As the Wiener process is equal to the sum of its increments $W_t = \int_0^t dW_s$, the integral in equations (2.15) and (2.20) can be evaluated as

$$\int_0^T W_t dt = \int_0^T \int_0^t dW_s dt = \iint_{0\le s\le t\le T} dt dW_s = \int_0^T (T-s)dW_s$$

The Itô integral, being a linear combination of independent normally distributed random variables, is also normally distributed. Because of the martingale property, it has zero mean. Calculations using the property of isometry find the variance $\int_0^T (T-s)^2 ds$. Since all increments of the Wiener process are normally distributed, i.e. $W_t - W_0 \sim \mathcal{N}(0,t)$, the Wiener process itself is normally distributed. As the sum of two normally distributed random variables

$$\int_0^T t dW_t \sim \mathcal{N}\left(0, T^2 + \frac{T^3}{3}\right). \tag{2.24}$$

2.2.2 Martingales

Stochastic processes where the expectation of a future value at any time is the current value of the process are called martingales. All Itô integrals belong to this class of stochastic processes. The Wiener process is also a martingale. There are inequality relations and conditions of convergence known for martingales, which automatically are true for the stochastic integrals.

Formally, a sequence of random variables $\xi_1, \xi_2, \ldots$ is called a **martingale** with respect to a filtration $\mathcal{F}_1, \mathcal{F}_2, \ldots$ if

1. ξ_n is integrable for all $n \in \mathbb{N}$
2. $\xi_1, \xi_2, \ldots$ is adapted to $\mathcal{F}_1, \mathcal{F}_2, \ldots$
3. $\mathrm{E}\big(\xi_{n+1}|\mathcal{F}_n\big) = \xi_n$ for all $n \in \mathbb{N}$

Definitions of these properties can be found in Appendix (A.2).

A random variable τ with values in the set $\{1, 2, \ldots, \} \cup \{\infty\}$ is called a **stopping time** if for each n $\{\tau = n\} \in \mathcal{F}_n$. The first time a stochastic process hits a certain value is one example of a stopping time.

If a process X has a sequence of stopping times τ such that $\lim_{n\to\infty} \tau_n = \infty$, and the stopped sequence is a martingale for each τ_n X is called a **local martingale**. One method of solving stochastic differential equations relies on local martingales. All martingales are local martingales but only bounded local martingales are martingales.

2.2.3 Solving a Stochastic differential Equation

Returning to stochastic differential equations with the knowledge of how to make sense of the $dW(t)$-term, it is possible to define what a solution to equation (2.3) is.

An Itô process $\xi(t)$ with $\mathcal{F}_0$-measurable initial condition ξ_0 is a solution to the stochastic initial value problem

$$\begin{cases} d\xi(t) = f\big(\xi(t)\big)dt + g\big(\xi(t)\big)dW_t \\ \xi(0) = \xi_0 \end{cases} \tag{2.25}$$

if

$$\xi(T) = \xi(0) + \int_0^T f\big(\xi(t)\big)dt + \int_0^T g\big(\xi(t)\big)dW_t. \tag{2.26}$$

The stochastic process f must be adapted to $\mathcal{F}_t$ and $\int_0^T |f(t)|dt < \infty$ a.s., and the stochastic process g must be possible to approximate with random step functions.

If f and g are Lipschitz continuous and ξ_0 is a $\mathcal{F}_0$-measurable random variable the initial value problem in equation (2.25) has a solution $\xi(t)$, $t \geq 0$. It is a unique solution in the sense that if $\eta(t)$, $t \geq 0$ is another Itô process satisfying the same initial value problem $\eta(t)$ is a.s. identical to $\xi(t)$, i.e. $\mathrm{P}\big(\xi(t) = \eta(t)\ \forall\ t \geq 0\big) = 1$.

A solution to a stochastic differential equation can have a maximum time of existence. This time, τ, is called the explosion time and is the stopping time $\lim_{t\to\tau} X_t = \infty$ for a stochastic process X_t that solves the differential equation. (Brz99)

Aside from calculations similar to the ones used for deterministic differential equations, a stochastic differential equation can be solved by formulating the Martingale Problem. For a one-dimensional diffusion process, this is done by defining two stochastic processes:

$$M_t = X_t - X_0 - \int_0^t b(X_s)ds \tag{2.27}$$

$$\Lambda_t = M_t^2 - \int_0^t \sigma^2(X_s)ds \tag{2.28}$$

If the processes M_t and Λ_t are both local martingales, X is a solution to the stochastic differential equation

$$X(t) - X(0) = \int_0^t b(X_s)ds + \int_0^t \sigma(X_s)dWs. \tag{2.29}$$

Since the Itô integral is a martingale, the process

$$M_t = X(t) - X(0) - \int_0^t b(X_s)ds \tag{2.30}$$

must also be a martingale in order for equation (2.29) to be true. By squaring and using the isometry properties of Itô integrals

$$M_t^2 = \left(X(T) - X(0) - \int_0^t b(X_s)ds\right)^2 = \left(\int_0^t \sigma(X_s)ds\right)^2 = \int_0^t \sigma^2(X_s)ds \tag{2.31}$$

which means

$$\Lambda_t = M_t^2 - \int_0^t \sigma^2(X_s)ds \tag{2.32}$$

is also a martingale when X solves (2.29). As all martingales, M_t and Λ_t are local martingales and $X(t)$ solves the martingale problem.

2.3 Convergence of stochastic processes

Suppose there is a sequence of random variables $(\xi_n)_{n\in\mathbb{N}}$, a random variable X on the probability spaces $(\Omega_n, \mathcal{F}_n, \mathrm{P}_n)$ and $(\Omega, \mathcal{F}, \mathrm{P})$, and a continuous, bounded function f. Then, if

$$\lim_{n\to\infty} \mathrm{E}_n\big(f(\xi_n)\big) = \mathrm{E}_n\big(f(\xi)\big) \tag{2.33}$$

the sequence (ξ_n) is said to **converge in distribution** to ξ, and if

$$\lim_{n\to\infty} \int f(x)\mathrm{P}_n(dx) = \int f(x)\mathrm{P}(dx) \tag{2.34}$$

the probability measures P_n is said to **converge weakly** to P. With the expectation E_n corresponding to P_n, if the process convergences in distribution, it also converges weakly.

If $\lim_{n\to\infty}\Big(\mathrm{P}\big(|\xi - \xi_n| > \varepsilon\big) = 0\Big)$ for all $\varepsilon > 0$ the sequence is said to **converge in probability** to ξ. A sequence that converges in distribution will also converge in probability, but the reverse is not necessarily true.

A sequence of probability measures on a metric space is **tight** if, for every $\varepsilon > 0$, there is a n_0 and compact set K such that $\mathrm{P}_n(K) > 1-\varepsilon$ for every $n > n_0$. Prohorov theorem states that in a complete, separable metric space, a sequence of random variables contains a weakly convergent subsequence if and only if it is tight.

2.3.1 Convergence of Martingales

Let ξ_n be a series of observations of a random variable ξ, where the observations gets closer to the true value of ξ with time. Then $\xi_n = \mathrm{E}\big(\xi|\mathcal{F}_n\big)$, which means that ξ_n is a martingale converging to ξ. Any martingale which is uniformly integrable, i.e. for all $\varepsilon > 0$ there exists a $M > 0$ such that $\int_{\{|\xi_n|>M\}} |\xi_n| d\mathrm{P} < \varepsilon$, converges to an integrable random variable.

Uniform integrability is a sufficient and necessary condition for martingales to converge in L^1. By Chebyshev's inequality, convergence in L^1 implies convergence in probability and convergence in distribution as well.

For a convergent process the limit $\lim_{n\to\infty} \mathrm{E}\big(|\xi_n - \xi|\big) = 0$. From Chebeshev's inequality

$$\mathrm{P}\big(|\xi - \mu| \geq k\sigma\big) = \frac{1}{k^2} \tag{2.35}$$

for any $k \in \mathbb{R}$ and any stochastic process ξ with $\mathrm{E}(\xi) = \mu$ and $\mathrm{Var}(\xi) = \sigma^2$. For a convergent process ξ the expectation $\mathrm{E}(\xi_n - \mu) = \mathrm{E}(\xi_n - \xi)$. When choosing $k = \frac{\varepsilon}{\sigma}$ it is true for any ξ_n in the sequence that

$$\mathrm{P}\big(|\xi_n - \mu| \geq \varepsilon\big) = \frac{\sigma^2}{\varepsilon^2} = \frac{\mathrm{E}[(\xi_n - \mu)^2]}{\varepsilon} \geq \frac{\mathrm{E}[(\xi_n - \mu)]^2}{\varepsilon}$$

by the Cauchy-Schwartz inequality. Taking the limit,
$\lim_{n\to\infty} \mathrm{P}(|\xi_n - \mu| \geq \varepsilon) = 0$, which for uniformly convergent ξ_n is equivalent to $\lim_{n\to\infty} \mathrm{P}(|\xi_n - \xi| \geq \varepsilon) = 0$, proving that ξ_n is convergent in probability.

Chapter 3

Particle system models SOS and WASEP

A particle system consists of finitely or infinitely many particles, where every particle attempts to change states according to an independent Markov chain. Interactions between particles result in the next step for any single particle to depend on more than its current position. However, the system as a whole is Markovian. (Lig85)

The state space of a particle system is denoted with

$$\Omega = \{\text{particle states}\}^{\{\text{number of particles}\}}$$

and its evolution is described with a Markov generator.

The following Sections describe two particle systems, the weakly asymmetric simple exclusion process and the single step solid on solid process, and the relationship between them.

3.1 Exclusion Process

In an exclusion process, space is considered on a finite lattice with fixed positions. Each position can be either occupied or empty. Two particles at different positions cannot move simultaneously, and in a simple exclusion process, there can be at most one particle at any given position. A particle at position x waits for a time $t \sim \text{Exp}(1)$, after which it attempts to move

to position y with probability $p(x, y)$. If y is vacant, the particle moves to y; otherwise, it stays at x. A stochastic process η_t describing the state of the lattice, or the configuration of the system, at time t has value $\eta_t(x) = 1$ for all x that are occupied at time t, and $\eta_t(x) = 0$ for vacant x.

3.1.1 Weakly Asymmetric Simple Exclusion Process

In the Weakly Asymmetric Simple Exclusion Process (or WASEP), particles tend to move in one direction slightly more often than the other. Instead of describing the process with occupation variables η_t as in the previous Section, spin variables can be used to make calculations easier. Then $\sigma(x) = -1$ when x is vacant and $\sigma(x) = 1$ when x is occupied. The state space for the WASEP is $\Omega = \{-1, 1\}^{\mathbb{Z}}$, and the current spin configuration at time t is $\sigma_t = \big(\sigma_t(x), x \in \mathbb{Z}\big)$. (Ber97)

In this process, a particle will jump one step to the right with probability $\frac{1}{2}$ and one step to the left with probability $\frac{1}{2} + \sqrt{\varepsilon}$, where ε is a small number. The Markov generator for the WASEP is constructed as a sum of two generators for a Totally Asymmetric Simple Exclusion Process (TASEP), an exclusion process where particles can only move in a single direction. The generator for a TASEP to the right looks like

$$L^+ f(\sigma) = \sum_x \frac{1 + \sigma(x)}{2} \cdot \frac{1 - \sigma(x+1)}{2} \big[f(\sigma^{x,x+1}) - f(\sigma) \big], \tag{3.1}$$

where $\sigma^{x,y}$ is defined as

$$\sigma^{x,y}(z) = \begin{cases} \sigma(x) & if \quad z = y, \\ \sigma(y) & if \quad z = x, \\ \sigma(z) & \text{otherwise.} \end{cases} \tag{3.2}$$

On matrix form $\big[f(\sigma^{x,x+1}) - f(\sigma) \big]$ becomes

$$\begin{bmatrix} f\big(\sigma(2)\big) - f\big(\sigma(1)\big) & f\big(\sigma(1)\big) - f\big(\sigma(2)\big) & 0 & 0 & \cdots & 0 \\ 0 & f\big(\sigma(3)\big) - f\big(\sigma(2)\big) & f\big(\sigma(2)\big) - f\big(\sigma(3)\big) & 0 & \cdots & 0 \\ 0 & 0 & f\big(\sigma(4)\big) - f\big(\sigma(3)\big) & f\big(\sigma(3)\big) - f\big(\sigma(4)\big) & \cdots & 0 \\ 0 & 0 & 0 & f\big(\sigma(5)\big) - f\big(\sigma(4)\big) & \cdots & 0 \\ 0 & 0 & 0 & 0 & \ddots & \dots \end{bmatrix}. \tag{3.3}$$

As the only non-zero elements are on the main and upper diagonal for each element x, the only possible transition from x is to $x+1$. Also, since the only possible values of $\sigma(x)$ is 1 and -1, the product $\left(\frac{1+\sigma(x)}{2} \cdot \frac{1-\sigma(x+1)}{2}\right)$ will be zero unless x is occupied and $x+1$ vacant. The generator L^+ finds which particles can jump right in the exclusion process.

Similarly, the generator L^-, which finds the particles that can jump left, is defined as

$$L^- f(\sigma) = \sum_x \frac{1+\sigma(x)}{2} \cdot \frac{1-\sigma(x-1)}{2} \big[f(\sigma^{x,x-1}) - f(\sigma)\big] \tag{3.4}$$

The generator for the WASEP, L_ε, is defined by combining these two:

$$L_\varepsilon = \frac{1}{2}L^+ + \left(\frac{1}{2} + \sqrt{\varepsilon}\right) L^-, \tag{3.5}$$

where $\sqrt{\varepsilon}$ is called the strength of the asymmetry, which here is to the left. ε can be arbitrarily small. (Ber97)

3.1.2 Tagged Particle Process

The tagged particle process follows the motion of one particle during the evolution of an exclusion process, often the one closest to the right of the origin at time $t = 0$, i.e. the first particle encountered when going through all sites one at the time beginning at the origin. This process is a combination of two Markov processes: the exclusion process σ and the process describing the movement of the tagged particle. From the view of the tagged particle, the system is stationary at any time. The effect of σ on the tagged particle is to slow down its movement. (Lig85)

Let x_t^0 be the position of the tagged particle at time t. At time 0, the tagged particle is picked to be the one closest to the right of the origin: $x_0^0 = \min\{x \in \mathbb{Z}, x \geq 0, \sigma(x) = 1\}$. The state space for the tagged particle process is $\{(\sigma, x) \in \Omega \times \mathbb{Z} : \sigma(x) = 1\}$. The joint Markov Process (σ_t, x_t^0) has the generator

$$H_\varepsilon = \frac{1}{2}H^+ + \left(1 + \sqrt{\varepsilon}\right) H^-, \tag{3.6}$$

where $H^{\pm}$ is defined as

$$H^{\pm}f(\sigma,x) = \frac{1}{2}\sum_{x\neq x^0}\frac{1+\sigma(x)}{2}\cdot\frac{1-\sigma(x\pm1)}{2}\big[f(\sigma^{x,x\pm1},x^0)-f(\sigma,x^0)\big] + \frac{1-\sigma(x^0\pm1)}{2}\big[f(\sigma^{x,x\pm1},x^0\pm1)-f(\sigma,x^0)\big]. \quad (3.7)$$

The first part of this generator describes the evolution of all particles except the tagged one, and for those particles, $H^{\pm}$ behaves like $L^{\pm}$. The second line of equation (3.7) represents the movement of the tagged particle. The probability of particle movement in either direction is 0 if the neighbouring spot is occupied. (Ber97)

3.2 Single Step Solid on Solid Process

The Single Step Solid on Solid process (SOS) is a model for surface growth in which particles are deposited on other particles or evaporate from a material. It is related to the Ising model, which describes how the spin of atoms in a magnetic material changes when subjected to an external magnetic field. The border between the two possible states – the microscopic interface – is represented by a single-valued function $\zeta : \mathbb{Z} \to \mathbb{Z}$. Assume ζ models the growth of a crystal, then $\zeta(x)$ is the height of the growing crystal at position x. The process has a single step constraint, $|\zeta(x+1)-\zeta(x)| = 1$. Independent of each other, local minima change to local maxima with rate $\frac{1}{2}+\sqrt{\varepsilon}$ and local maxima become minima with rate $\frac{1}{2}$.

The state space for the SOS process is

$$\hat{\Omega} = \{\zeta \in \mathbb{Z}^{\mathbb{Z}} : \forall\, x \in \mathbb{Z}\ |\zeta(x+1)-\zeta(x)| = 1\}. \quad (3.8)$$

Its evolution is governed by the Markov generator

$$\hat{L}_{\varepsilon}(\zeta) = \sum_x c^{+}(x,\zeta)\big[f(\zeta+2\delta_x)-f(\zeta)\big] + c^{-}(x,\zeta)\big[f(\zeta-2\delta_x)-f(\zeta)\big], \quad (3.9)$$

where

$$c^{+} = \begin{cases} \frac{1}{2}+\sqrt{\varepsilon} & \text{if} \quad \zeta(x+1)-2\zeta(x)+\zeta(x-1) = 2, \\ 0 & \text{otherwise.} \end{cases} \quad (3.10)$$

and

$$c^- = \begin{cases} \frac{1}{2} & \text{if} \quad \zeta(x+1) - 2\zeta(x) + \zeta(x-1) = -2, \\ 0 & \text{otherwise.} \end{cases} \tag{3.11}$$

c^+ is only non-zero when $\zeta(x)$ is a local minimum, and c^- is non-zero at local maxima only. In the sum in equation (3.9), only the current x is significant, and for all other values $f(\zeta + 2\delta_x) - f(\zeta) = 0$.

3.2.1 Initial Distributions to the SOS

There are requirements for the initial distribution of ζ to ensure its convergence. For the family $\{\mu_\varepsilon\}_{\varepsilon>0}$ of probabilities on $\hat{\Omega}$ to be an initial distribution to the SOS, it has to satisfy three conditions. These distributions are called near-stationary.

ζ should have the same scaling as a Wiener process, which means that $\zeta^\varepsilon(r) = \sqrt{\varepsilon}\zeta(\varepsilon^{-1}r)$ has the same properties as ζ. The first condition is the existence of a random function h_0 such that $\zeta^\varepsilon \Rightarrow h_0$ as $\varepsilon \to 0$ in the topology of $C(\mathbb{R})$.

The second condition sets a bound on the growth of ζ; it cannot grow faster than exponentially. Formally, for each $n \in \mathbb{N}$ there exists $a > 0$ and $c > 0$ such that for the expectation corresponding to the probability measure μ_ε

$$\sup_{x\in\mathbb{Z}} e^{-a\varepsilon|x|}\mathrm{E}(e^{-n\sqrt{\varepsilon}\zeta(x)}) \leq c. \tag{3.12}$$

The third condition provides an estimate which implies that the initial distribution is Hölder continuous with exponent $< \frac{1}{2}$. This level of roughness appears in Brownian motion. For each $n \in \mathbb{N}$ and $\varepsilon > 0$ there exists $a > 0$ and $c > 0$ such that

$$\mathrm{E}\left(\sqrt{\varepsilon}[\zeta(x) - \zeta(y)]\right)^{2n} \leq ce^{a\varepsilon(|x|+|y|)}\left(\varepsilon|x-y|\right)^n. \tag{3.13}$$

Assume m is a Hölder continuous function on $\mathbb{R}$ with $\alpha \geq \frac{1}{2}$ that fulfils

the growth condition $|m(r)| \leq a\big(1+|r|\big)$ for all $r \in \mathbb{R}$ and some $a > 0$. Further assume the increments, $\zeta(x+1) - \zeta(x) \in \{1, -1\}$, are independent and that the distribution μ_ε of the marginals $\big[\zeta(x+1) - \zeta(x)\big]$ depend on $m(r)$ as

$$\mu_\varepsilon\big(\zeta(x+1) - \zeta(x)\big) = \frac{1}{\sqrt{\varepsilon}}\big[m(\varepsilon x) - m(\varepsilon(x-1))\big]. \tag{3.14}$$

In this case, the distribution μ_ε fulfils the conditions for an initial distribution of the SOS. The probability of the increment $\zeta(x+1) - \zeta(x)$ depends on a function of x and $x-1$.

The conditions in (Ber97) are satisfied for a deterministic ζ_0 where

$$\zeta_0(x) = \begin{cases} y & \text{for even } x, \\ y+1 & \text{for odd } x. \end{cases} \tag{3.15}$$

This ζ_0 is known as the flat initial condition. Another initial distribution that fulfils the above conditions is Brownian motion - a random walk. Their combination, the flat $\rightarrow$ Brownian initial condition, which resembles the flat for $x \leq 0$ and Brownian motion for $x > 0$, also satisfies the requirements for an initial distribution.

Later research has found a valid initial condition that is not near-stationary, the wedge initial condition $\zeta_0 = |x|$. However, by using the Gärtner transform (equation(5.49)) and scaling with $\frac{\varepsilon^{-1/2}}{2}$ the transformed process $\frac{\varepsilon^{-1/2}}{2} Z_\varepsilon$ converges to $\delta_{x=0}$, and the first condition is satisfied. Further, it can be shown that this $Z_\varepsilon(t, \cdot)$ satisfies the second and third condition for all times $t > 0$ and the family of solutions does converge when $t \rightarrow 0$. Similar arguments can be made to prove that the scaled and transformed process satisfies the three requirements for the wedge-Brownian initial distribution, where $\zeta_0(x) = -x$ for $x \leq 0$ and a random walk for positive x, and the wedge-flat initial condition, where $\zeta_0(x) = -x$ for $x \leq 0$ and oscillates between 2 values for positive x. The six initial conditions mentioned above correspond to the six fundamental growth geometries in the KPZ class. (Cor11)

3.3 Relationship between WASEP and SOS

The two models described above are related and can be derived from each other. The probability for a particle to move left in the WASEP is the same

as the probability of deposition in the SOS. Assuming the initial distribution satisfies the necessary conditions, SOS can be obtained from WASEP as in equation (3.16). Here ζ is the SOS, σ is the WASEP, and x_t^0 is the tagged particle.

$$\zeta_t(x) = \begin{cases} \sum_{x_t^0 < y \leq x} \sigma_t(y) - x_t^0 & \text{if} \quad x > x_t^0, \\ -\sum_{x < y \leq x_t^0} \sigma_t(y) - x_t^0 & \text{if} \quad x < x_t^0, \\ -x_t^0 & \text{if} \quad x = x_t^0. \end{cases} \tag{3.16}$$

When $x > x_t^0$, the position x is to the right of the tagged particle. The height of the interface $\zeta(x)$ is the sum of the values of σ for all positions y between the tagged particle and the current x subtracted by the position of the tagged particle.The distance from the tagged particle to any x puts a maximum limit on the value of $\zeta(x)$. Since the state space for σ is $\Omega = \{-1, 1\}^{\mathbb{Z}}$, $\zeta(x)$ could reach any integer its state space is $\mathbb{Z}^{\mathbb{Z}}$.

For any $x > x_t^0$ the increment

$$\big|\zeta(x) - \zeta(x+1)\big| = \left| \Big(\sum_{x_t^0 < y \leq x} \sigma(y) - x_t^0 \Big) - \Big(\sum_{x_t^0 < y \leq x+1} \sigma(y) - x_t^0 \Big) \right| = \big|\sigma(x+1)\big| = 1. \tag{3.17}$$

Similar results can be obtained for $x < x_t^0$, which means the single step constraint for ζ is satisfied for all x.

To obtain the WASEP from the SOS set $\sigma_t(x) = \zeta_t(x) - \zeta_t(x-1) = \nabla\zeta_t(x)$. Because of the single step constraint the possible values of σ are $\{-1, 1\}$, which gives the state space $\{-1, 1\}^{\mathbb{Z}}$.(Ber97)

The SOS is evaluated at different points on the lattice than the WASEP. If the sites of the WASEP are $\mathbf{x} = (\dots, x-1, x, x+1, x+2, \dots)$ the sites for the associated SOS are $\mathbf{x}' = (\dots, x - \frac{3}{2}, x - \frac{1}{2}, x + \frac{1}{2}, x + \frac{3}{2}, \dots)$. In the literature, the sites in both discrete lattices are denoted with the same x.

Chapter 4

Simulations

Because of the relationship between the WASEP and the SOS, it was sufficient to simulate only the WASEP and calculate the SOS from the result. The simulations are made using a graphical visualization of a Simple Exclusion Process described in (Cor11), which is explained in Section 4.1. Section 4.2 contains simulations of small systems with high asymmetry and explores the particle dynamics and relation between models. With high values of ε, the modelled exclusion process is no longer weakly asymmetric but rather an example of the Asymmetric Simple Exclusion Process (ASEP). The ASEP and the WASEP have the same relationship to the SOS. The simulations in Section 4.3 are done for larger systems, and the asymmetry is inversely proportional to the system size. Here, long-term behaviour is compared for different system sizes and initial conditions.

4.1 Method

Figure (4.1) shows a sketch of the graphical representation of a WASEP process. A lattice with discrete positions where a particle can be located is situated on the x-axis. Time is represented on the y-axis. For each site in the lattice, two Poisson processes are attached: L describing jumps one step to the left and R describing jumps one step to the right. In figure 4.1, these Poisson processes are illustrated with purple (L) and green (R) arrows. Their positions on the y-axis represent the time a jump can occur. In order for the state of the particle system to change at any given time, the current position must be occupied, and the relevant neighbour must be empty.

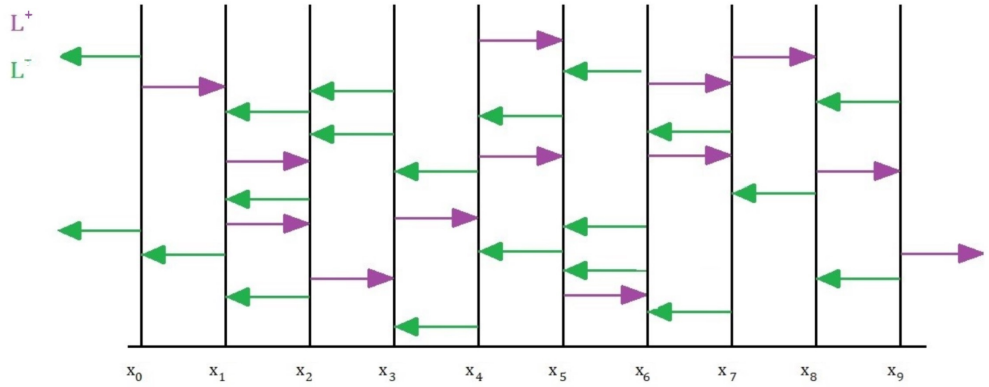

Figure 4.1: A graphical representation on the WASEP. Time is on the y axis, and particle locations are on the x axis. The arrows represent times when it is possible to jump from one location to the adjacent

In figure 4.2 A, 5 particles have been added to the system in figure 4.1. The tagged particle, at site x_1, is red. The other four, at x_2, x_5, x_7 and, x_8, are blue. The first jump happens at time t_1 when the particle at x_7 jumps to x_6. Between t_1 and t_2, the particles at x_5 and x_6 attempt to jump but find the neighbouring space occupied at those times. Figure 4.2 A shows the individual particles at different times, and in figure 4.2 B, the paths they take are included.

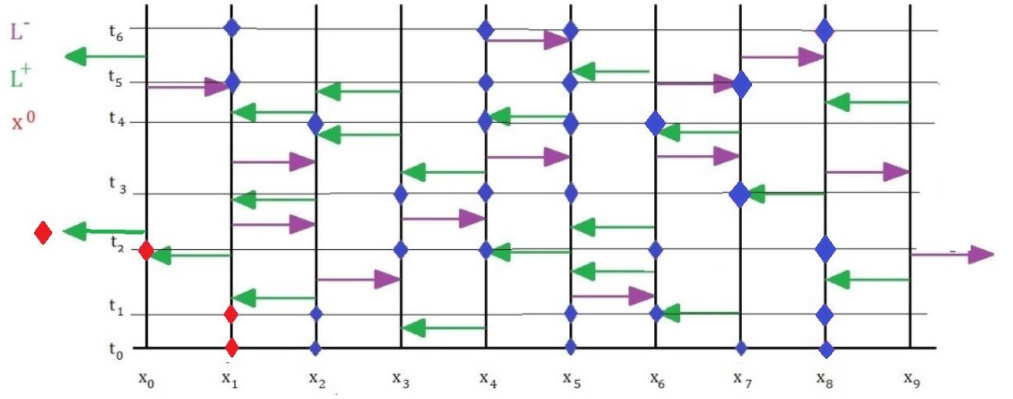

A. The position of the particles at various times in the simulaton

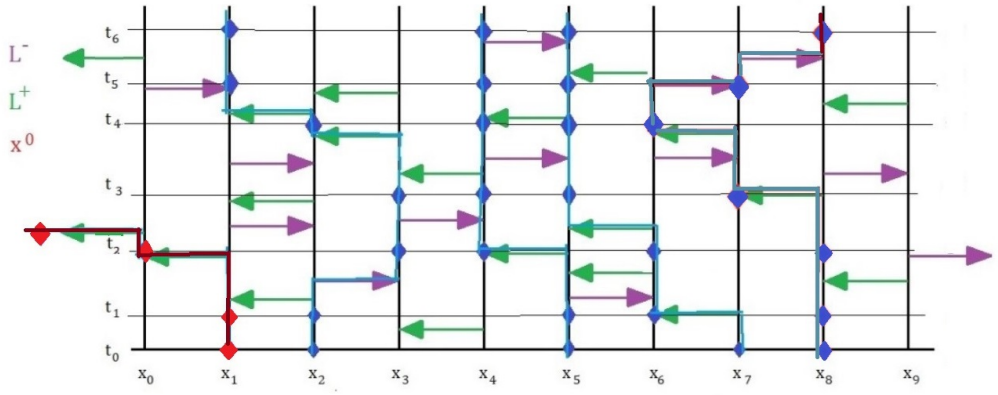

B. The paths of the individual particles

Figure 4.2: A simulation of the particle system in figure 4.1. The blue dots represent particles. The tagged particle, marked in red, is the one furthest to the left at time 0. At each time step t_0 to t_6, the position of each particle is marked. In the right figure, the paths of all particles are drawn.

The first step in the simulation is to generate the two processes L and R with intensities $\frac{1}{2}+\sqrt{\varepsilon}$ and $\frac{1}{2}$ respectively. The intensities are normalized and calculated as the probability of going in either direction for a Poisson process with intensity 1. When $\varepsilon \to 0$, this is close to the true process and conserves the ratio between left and right. For larger ε, two processes with different intensities are simulated instead. The processes are stored in a variable called a *jump* that contains the time a particle can shift state, its position before the state shift and the direction it attempts to move in.

In Section 4.2, particles can enter and exit the system, and jumps are generated for every position in the lattice, plus one outside that represents particles entering the system. In Section 4.3, borders are assumed to be impassable, and jumps are only generated for the points inside the lattice. The jumps for all positions are sorted by time.

// Initialize jumps

for all positions i
    $time = 0$;
    while $time < max\_time$ // generate L
        t = −log(1− u) // $u \sim U(0,1)$, $t \sim Exp(1)$
        $time = time$ + t;
        if c = rand < $\frac{q}{q+p}$ // q = P(left), p = P(right)
            $dir = -1$;
        else
            $dir = 1$;
        end
        new jump with position i, time $time$ and direction dir
    end
end

The configuration of the WASEP is represented by a vector of size n called *wasep*. The initial value of the tagged particle x0_t is the position of the first positive element in this vector. In Section 4.2, the WASEP and SOS are simulated simultaneously, and the WASEP is represented by spin variables $\{-1, 1\}$. In Section 4.3, the SOS is calculated afterwards, and occupation variables $\{0, 1\}$ were used instead to simplify calculations of the mean occupancy of any site in the WASEP.

The simulation of the particle system begins when *jumps* and *wasep* are initialized. It iterates through the list of jumps, each time processing the as yet untreated jump with the lowest time value. After checking the feasibility of the particle movement, the configuration vector *wasep* updates. In Section 4.2, the initial number of particles is 50, and the size of the lattice is 100. Particles can move in and out of the lattice. For similar probabilities of successful movement inside and across the borders, the site just outside is assumed to be occupied with probability 0.5. In Section 4.3, because of the assumption of impassable boundaries, it is only the last if-clause in the pseudo code below, concerning the interior points, that is active.

```
// step
while jumps not empty
      jump = next jump in the list;
      from = jump.position;
      to = from + jump.direction;
      if from = n + 1 //entering particle
            if wasep[to] == −1 and rand < 0.5
                  wasep[to] = 1 //to = 0 or to = n
            end
      end
      if (from = n and direction > 0) or (from = 1 and direction < 0)
      // exiting particle
            if wasep[from] == 1 and rand < 0.5
                  wasep[from] = −1;
            end
      end
      if wasep[from] == 1 and wasep[to] == −1
            wasep[from] = −1;
            wasep[to] = 1;
     end
end
```

The SOS can be calculated directly from the WASEP using equation (3.16). As an element of the WASEP is equal to the slope between two points in the SOS, the lattice used for a simulation is not the same for the two particle

systems. If the WASEP is simulated over n points, the corresponding SOS requires $n+1$.

4.2 Simulations on small systems

To observe how the dynamics of the particle systems at the microscopic level, they are simulated with few sites and high asymmetry and animated in Java. The images in figures 4.3, 4.4, 4.5, 4.6, and 4.7 are taken from these animations. In these simulations, the number of sites for the exclusion process is 100, and the initial number of particles is 50. The corresponding number of sites for the SOS is 101. Particles can enter the system at both borders and at any one time, it is assumed the site just outside the border is occupied with a probability of 0.5. The asymmetry in these simulations is to the left, but the figures are flipped to show a growing process. The exclusion process modelled in this Section is the ASEP.

Figure 4.3 shows a Section of the system four times at the beginning of a simulation of the SOS with $\varepsilon = 0.25$. The discrete system with particles as blue dots is to the left, and the linear interpolation of the surface is added to the right images. Image A and its right neighbour show the initial distribution of the particles. This distribution is the flat initial condition from Section 3.2, which is known to satisfy the criteria in (Ber97). In image B of this figure, the first deposition has occurred. The neighbouring positions to the one which changed are now neither local minima nor maxima. The height of these two positions will stay at the same level until the system changes so that they are local extreme points again, after which change will be possible. In image C, a short time has passed, and deposition or evaporation has occurred in several places. The bottom image, D, shows the state of the system after some more time. 49 of the 101 sites in the simulated system are shown in figure 4.3.

In figure 4.4, two simulations of the SOS with flat initial conditions are depicted. In the left image, the asymmetry is $\varepsilon = 0.25$, and in the right, $\varepsilon = 0.75$. The process is recorded in 5 equidistant points in time, with the yellow line being the initial condition and the red being the distribution at the end of the simulation. The times in between are shown in different shades of orange; the darker the shade, the more time has passed in the simulation. It is clear that a higher asymmetry ε leads to faster growth.

The premise of figure 4.5 is similar to figure 4.4 but with an initial condition $|x|$, the wedge initial condition. In the beginning, the height function is V-shaped, and with increasing simulation length, the shape gradually becomes rounder.

Figures 4.6 and 4.7 show the same processes as figures 4.4 respectively 4.5 but includes the underlying exclusion process. In figure 4.6, the process with a flat initial condition is shown in the beginning and after some time with different asymmetries. Figure 4.7 shows 3 points in time for the process with wedge initial condition. The configuration of the WASEP is depicted on a line, with dots on the occupied sites. The tagged particle is green, and all the others are blue. Since particles can enter and exit the system, the tagged particle is not always the one furthest left or even in the visible part of the system. The connection between the two particle systems is visible in these two figures. The slope of the SOS is 1 when there is a particle in the site to its right and -1 when there is no particle. The wedge-shaped initial condition of the SOS corresponds to all particles being on one half of the lattice for the ASEP. In the flat initial condition, every other site is occupied.

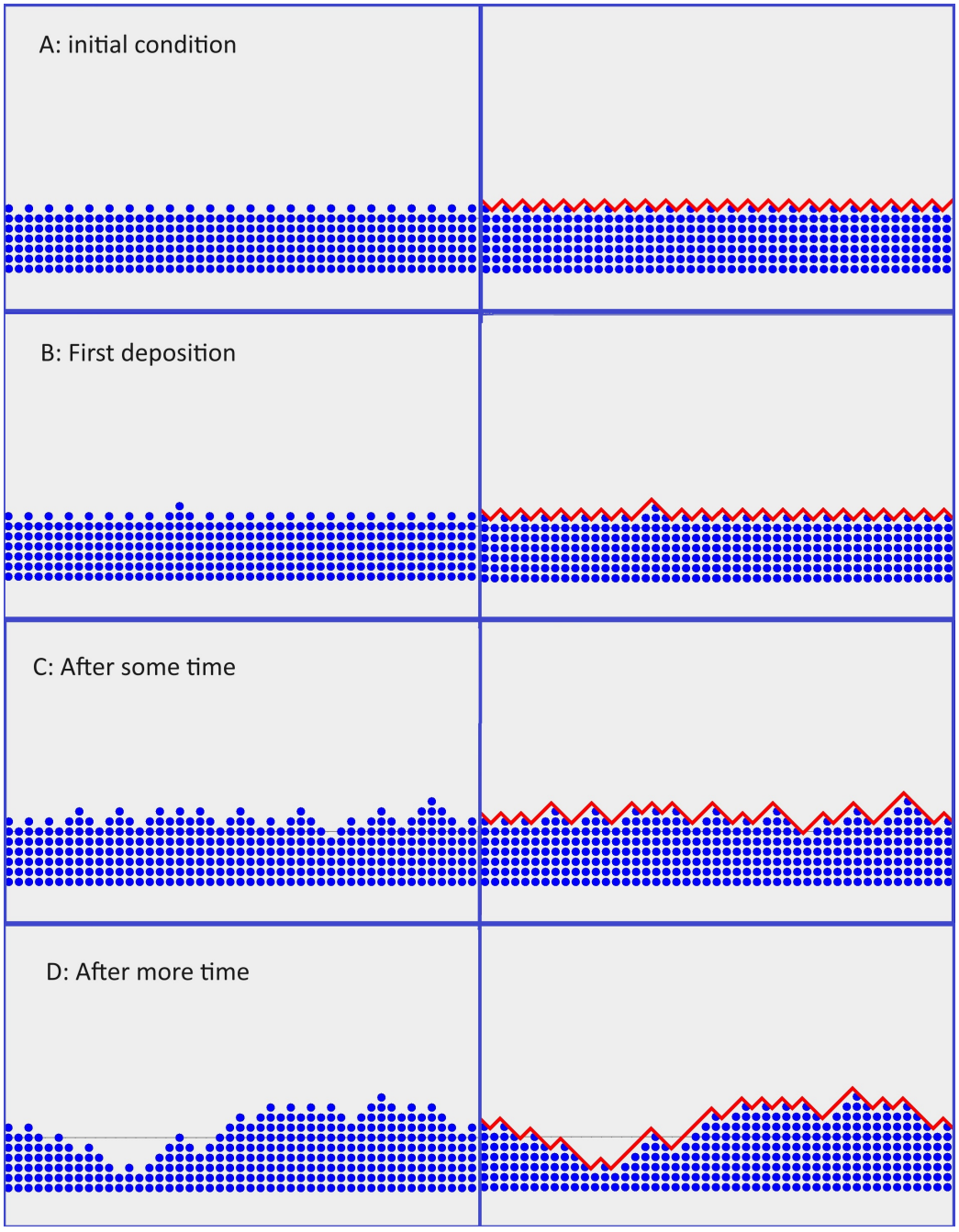

Figure 4.3: Several time points when simulating the SOS with $\varepsilon = 0.25$. The left images show the particles, and the images to the right include the interpolated function. Image A shows the initial configuration. Image B is just after the first particle deposition. In image C, some time has passed, and image D shows the distribution at the end of the simulation

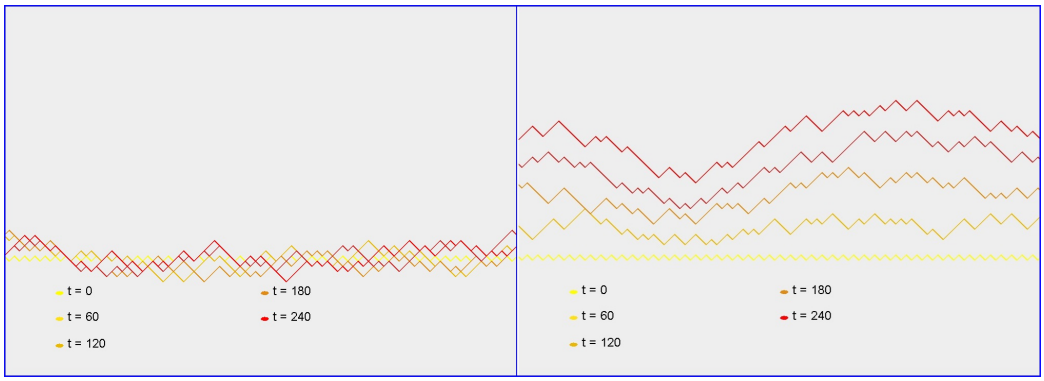

Figure 4.4: Two simulations of the SOS captured at 5 points in time. In the left image $\varepsilon = 0.25$, and in the right $\varepsilon = 0.75$

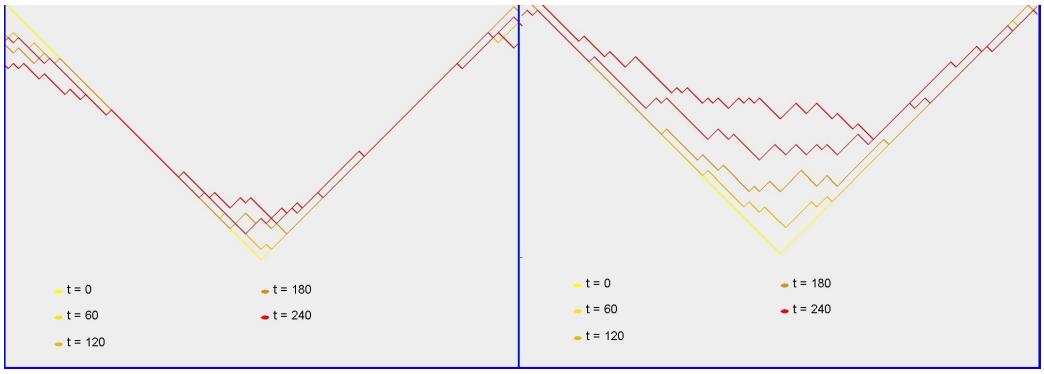

Figure 4.5: The SOS at five different time-points in one iteration with different ε and wedge initial condition

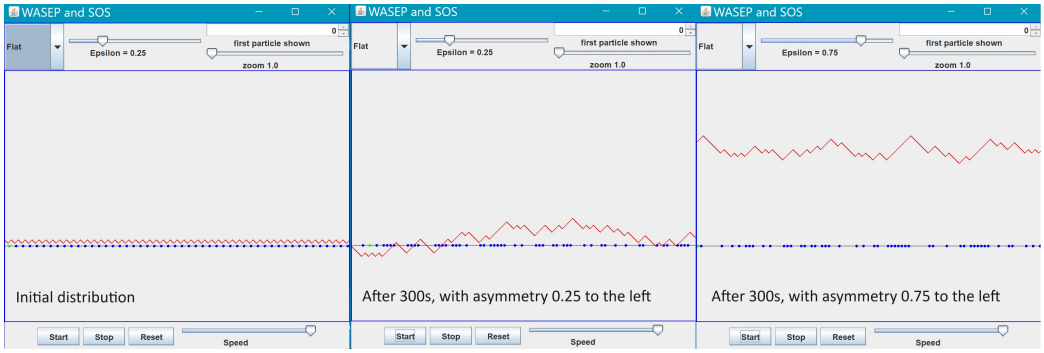

Figure 4.6: ASEP and SOS with flat initial condition and varying large ε

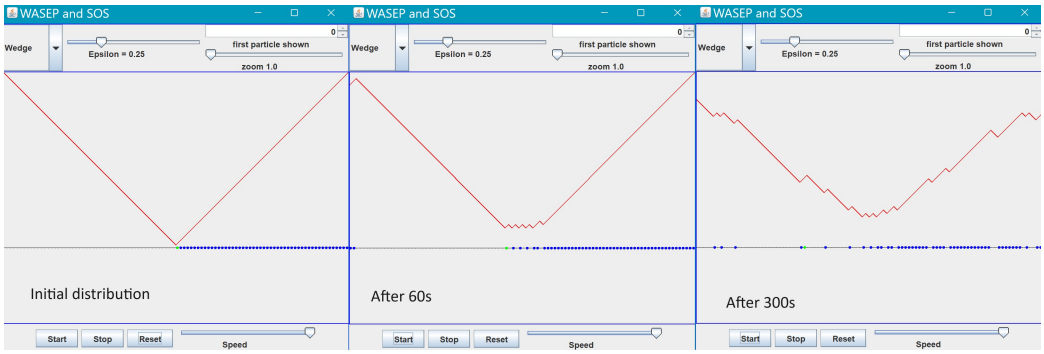

Figure 4.7: ASEP and SOS with wedge initial condition and varying large ε

4.3 Simulations on larger systems

The simulations in this Section show the long-term behaviour of the WASEP and SOS for particle systems with a number of sites N between 500 and 2500, varying numbers of particles and different initial distributions. They are run as $4N$ consecutive simulations of time $N/4$, with the initial condition of each being the result of the last one. In the majority of the simulations, the system size is $N = 1000$.

4.3.1 Simulation of the WASEP

After enough time, the mean distribution of particles in the WASEP reaches an equilibrium. The distribution is calculated as the probability for each site to be occupied at the end of a simulation.

The mean of the final distribution for 50 instances of the WASEP in a system with $N = 2000$ is shown in figure 4.8. In Figures A and B, the simulations have 200 particles, in Figures C and D they have 1000, and in E and F 1600. In the left figures (A, C and E), the WASEP is shown together with the least square approximation of a straight line in red.

After removing the linear dependence from the measured distribution, random noise remains. Figure 4.11 shows the spectra of the residual noise. The spectrum is relatively flat and varies around 0.003, which suggests that the noise is Normally distributed. This indicates that the stationary distribution of the WASEP can be approximated with a linear equation with added white noise.

Figure 4.8 compares the WASEP (blue) to a process composed of the line found with Least Squares approximation and Gaussian noise with the same standard deviation as the original WASEP (red). Images A, C and E show the WASEP with different number of particles, and images B, D and F the approximated process. The mean of the sum of the squared errors for these three approximations is 0.0024, 0.034, respectively 0.0051.

Looking at the Least Square estimated line for the WASEP at different points in time, the constant term is always the fraction of occupied sites. The slope initially changes to stabilize around a constant that depends on the number

of particles in the system. Figure 4.9 shows the estimated slope of the mean WASEP through time for a system with 1000 sites and 300 particles. It has been fitted with non-linear Least Squares to a line $y = m(1-2^{-t/k})$, where m is the final value of the slope and k determines how fast it converges. As seen in figure 4.10, the speed of convergence depends on the number of particles in the system. When half of the sites are occupied, convergence is faster than in systems where the difference between the number of occupied and empty sites is vaster.

Figure 4.12 shows the average position furthest right and furthest left reached by the tagged particle at different times for 8 systems with $N = 1000$ and between 200 and 900 initially evenly distributed particles. The asymmetry is to the left, and for all of the systems, the position furthest to the left reached is the left border at site 1. The most remote attainable position to the right seems to stabilize with time. Where it is depends on the initial number of particles. More sites are reachable for the tagged particle for a system with fewer particles. The variation of which position this is also greater for systems with fewer particles.

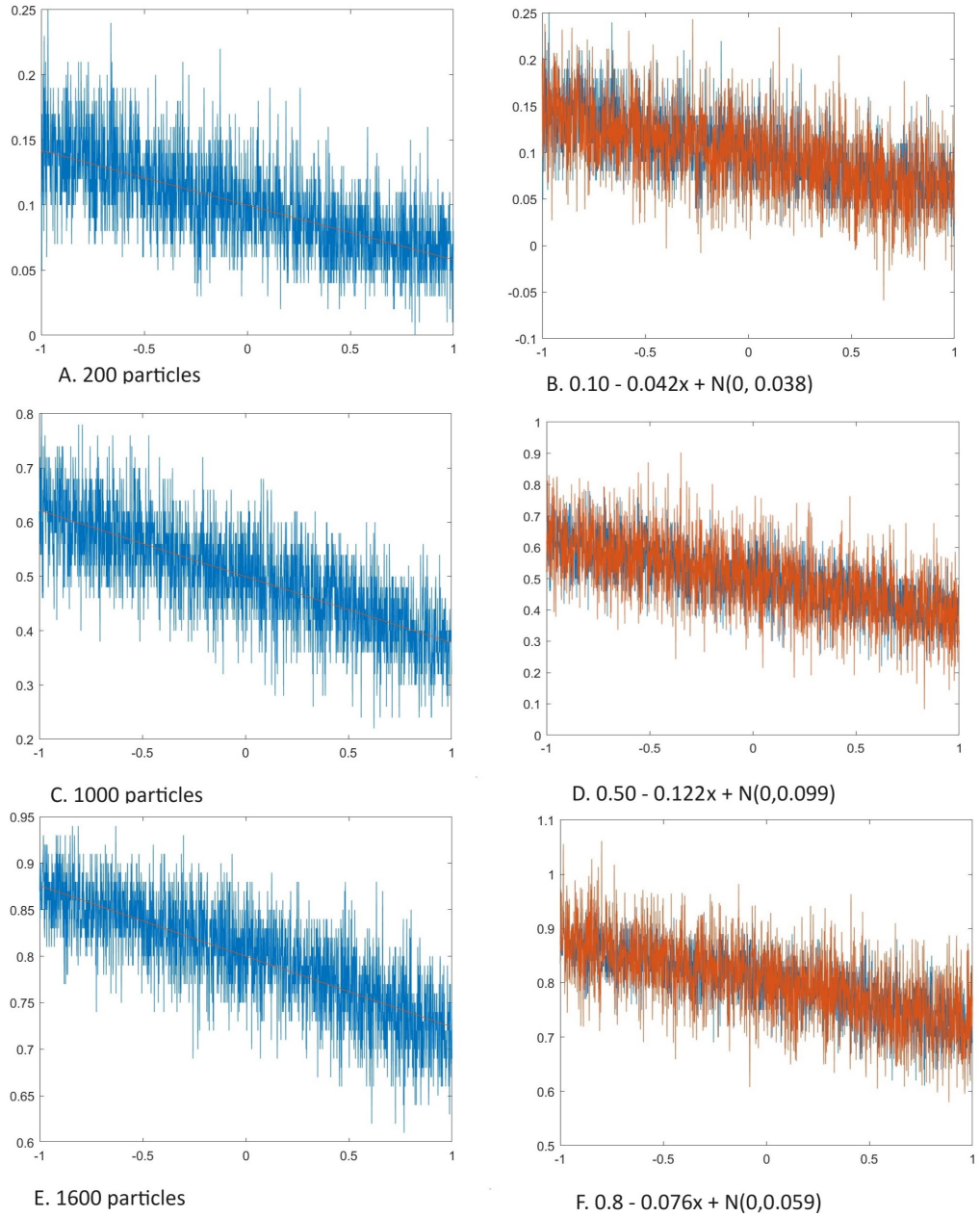

Figure 4.8: The likelihood of a particle to be at a site in the WASEP as an average of 200 iterations, with 2000 sites in total. The red line is the Least Squares estimate. The system in Figure A has 200 particles and shows the simulated process together with its approximation $0.10-0.042x+\mathcal{N}(0, 0.038)$ in Figure B. Figures C and D have 1000 particles, and the approximation $0.50 - 0.082x + \mathcal{N}(0, 0.083)$ and figure E and F have 1600 particles and the approximation $0.80 - 0.076x + \mathcal{N}(0, 0.059)$

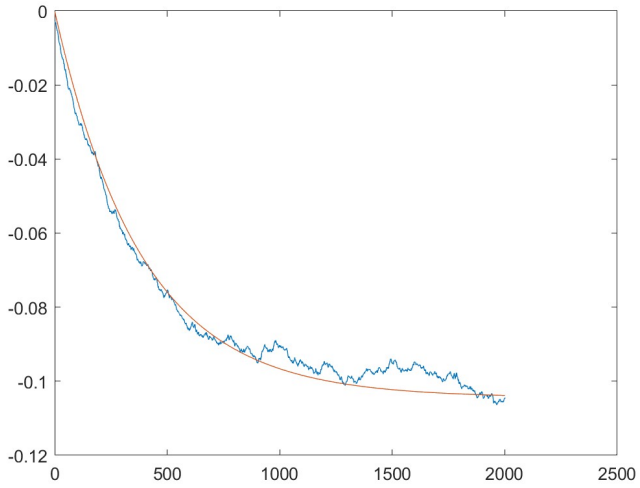

Figure 4.9: The slope of the Least Square estimate of the WASEP for a system with 1000 sites and 300 particles at different times and the estimated function of the slope in time. The slope of the WASEP converges.

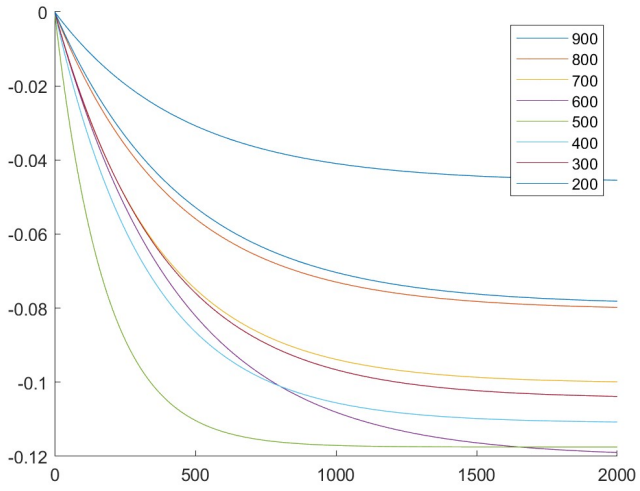

Figure 4.10: The estimated function of the slope in time for eight systems with 200 to 900 particles. The system with 500 particles converges faster than the ones with more particles, the system with 900 particles converges slowest

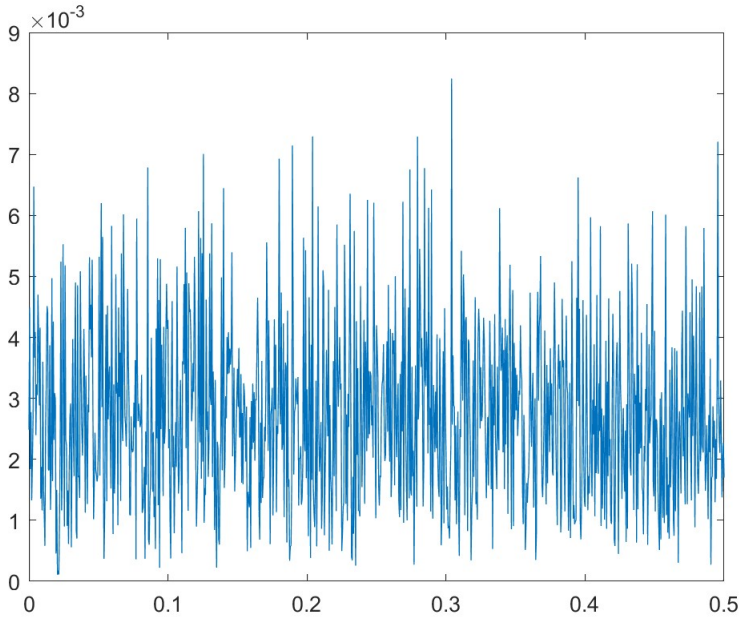

Figure 4.11: The spectra of the WASEP with 2000 sites and 1000 particles after the linear dependence was removed.

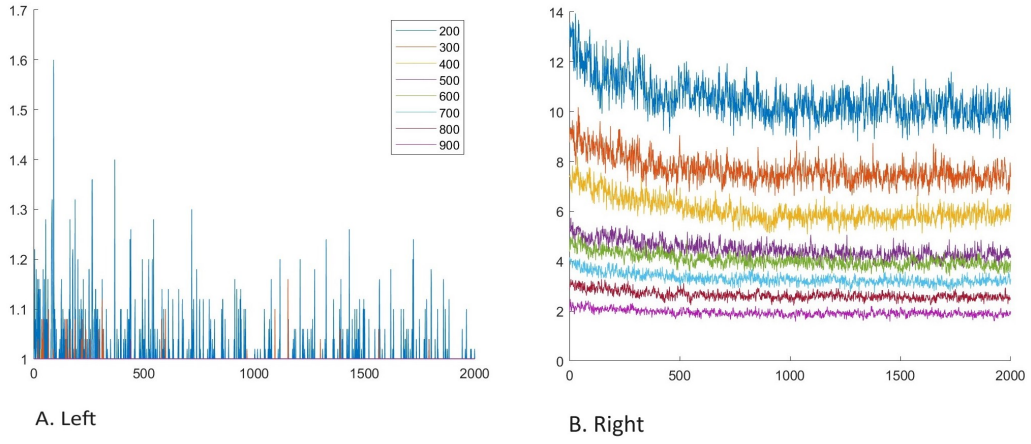

Figure 4.12: The position furthest to the left (A) and furthest to the right(B) for the tagged particle as an average of 50 iterations for a varying number of particles which were initially evenly distributed

4.3.2 Simulation of the SOS

To find the distribution of the SOS, equation (3.16) is implemented and applied to all iterations of the final configuration of the WASEP. After that, the mean height of the iterations of the SOS is computed.

Figure 4.13 shows the mean of the SOS at several points in time for the flat and the wedge initial conditions. Eventually, both reached a parabola of approximately the same height and stayed there.

Figure 4.14 shows the mean height of the final distribution of the SOS for 9 systems with $N = 1000$ and the number of particles varying between 100 and 900 together with the least squares estimate of a parabola. Initially, in all systems, the particles were evenly distributed. The residuals of the Least Squares fitting calculated as $\frac{1}{N}\sum(\zeta(x) - (ax^2 + bx + c))^2$ are recorded in table 4.1. Overall, the final distribution of the SOS is fairly well-described with a second-degree polynomial.

The mean variance of 50 iterations of the nine processes in figure 4.14 is recorded in table 4.2. The system with 500 particles has noticeably higher variance than, for instance, the systems with 100 or 900 particles. When the number of free sites is close to the number of occupied, there are more possible particle configurations as compared to systems with significantly more or fewer particles.

Figure 4.15 A shows the nine systems of figure 4.14 in the same plot. In the image, the final distributions (solid line) are compared to the initial ones (dashed line). The initial distributions on this scale are straight lines with the slope dependent on the number of particles in the corresponding exclusion process. In the equilibrium state, the lines have curved, but their endpoints remain the same.

Rotating the distributions in figure 4.15 by removing the linear dependence originating from the initial distribution, it transforms into the distribution in figure 4.16 A. The final distributions are parabolas of varying heights. The maximum height of the parabolas follows the same patterns as the variances, with the systems with low or high numbers of particles being shorter than the middle ones. The height of the distribution for the particle systems with

100 and 900 particles are relatively close, as are the systems 200 and 800, 300 and 700, and 400, 500 and 600. The maximum height of the SOS is recorded in the table 4.2. Normalizing by dividing by max height produces figure 4.16 B. After normalization, the stationary distribution of all SOS systems can be approximated by the same curve $1 - x^2$.

Similarly, figure 4.17 compares the stationary distribution for systems with different sizes N all with $\frac{N}{2}$ particles. Once again, normalization results in a $1 - x^2$ curve 4.17 B. This curve becomes much smoother with an increasing system size N.

Together, figures 4.17 and 4.16 suggest the equilibrium of the SOS to be $1 - x^2$ multiplied with a constant depending on N and the number of particles, and adjusted for the linear dependence from the initial distribution.

In figure 4.18, 10 instances of the SOS are shown for two systems. In 4.18 A the system has 2500 sites and 1250 particles and in 4.18 B there are 500 sites and 250 particles. The larger system is much smoother, and the different iterations seem to vary around a parabola. The smaller system shows no such common shape. At this level of the microscopic-macroscopic scale, the stochastic process dominates. In figure 4.19, the 500 site system is compared to a fifth of the 2500 site system where the processes have a similar structure. The difference comes from the endpoints. In image A, the boundary conditions $\zeta(1) = \zeta(N) = 0$ are absent.

Figure 4.20 shows part of one iteration of the SOS after it has stabilised. The first state is in blue. In the 2.5s following, successful jumps occurred 601 times. These are shown in green in figure 4.20, and the final distribution is black. Changes have happened more often at places where the average slope of the SOS is relatively flat.

Number of particles	100	200	300	400	500	600	700	800	900
Residuals	0.653	1.723	0.689	1.111	0.699	1.368	0.461	0.986	1.186

Table 4.1: Residuals of the Least Square estimate for the SOS of 50 iterations with 1000 sites and varying number of particles

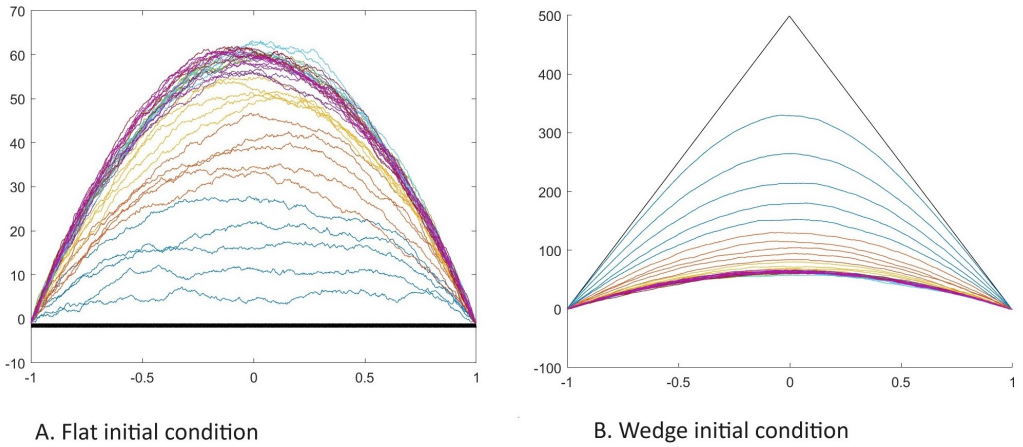

Figure 4.13: The mean of the SOS at various points in time for flat (A) and wedge (B) initial conditions. The 40 recorded times of the SOS are organized in 8 sequential groups, represented by different colours in the image, beginning with blue, red, and yellow and ending with purple.

Number of particles	100	200	300	400	500	600	700	800	900
Mean variance	53.5	92.4	120.5	168.9	176.1	150.6	132.7	111.0	92.3
Max height	17.5	43.4	53.7	59.6	61.4	60.7	51.2	44.0	25.4

Table 4.2: Mean variance of the SOS of 50 iterations with 1000 sites and a varying number of particles and the maximum height of the SOS in figure 4.16

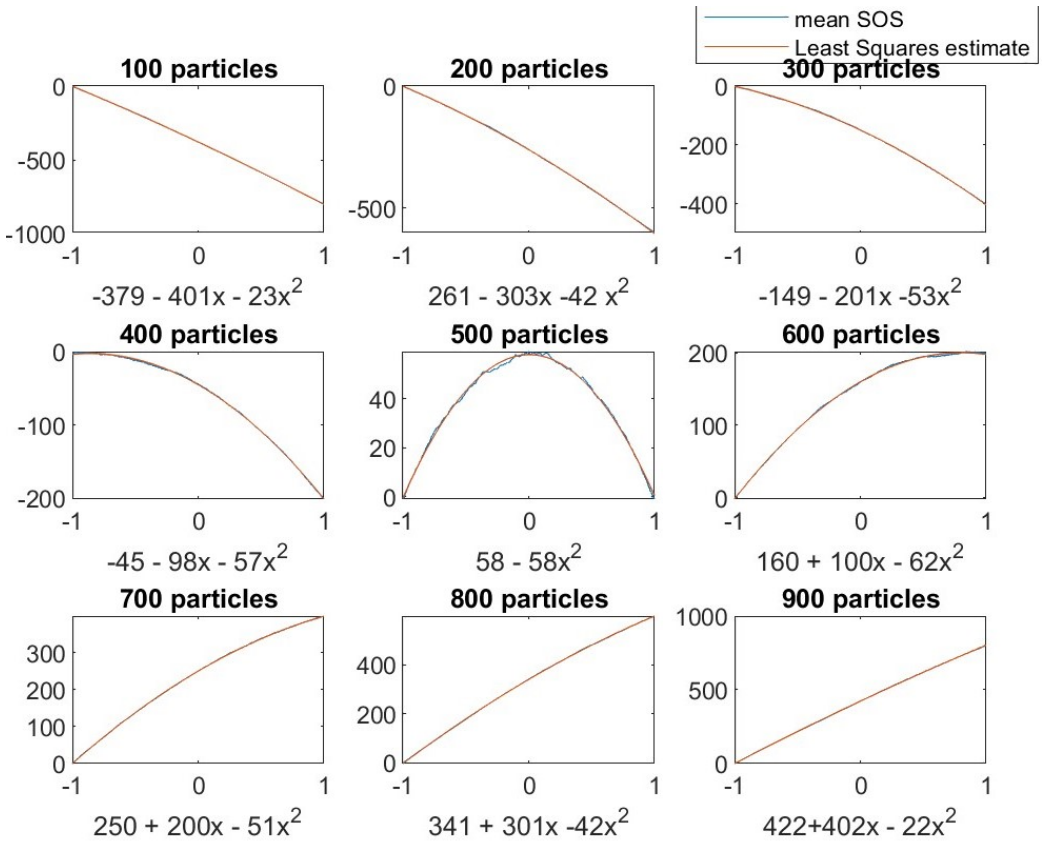

Figure 4.14: The final distribution of the SOS for a system with 1000 sites for a varying number of particles together with the approximation given by the Least Squares estimated second-degree polynomial. Residuals of the estimated polynomial can be found in table 4.1

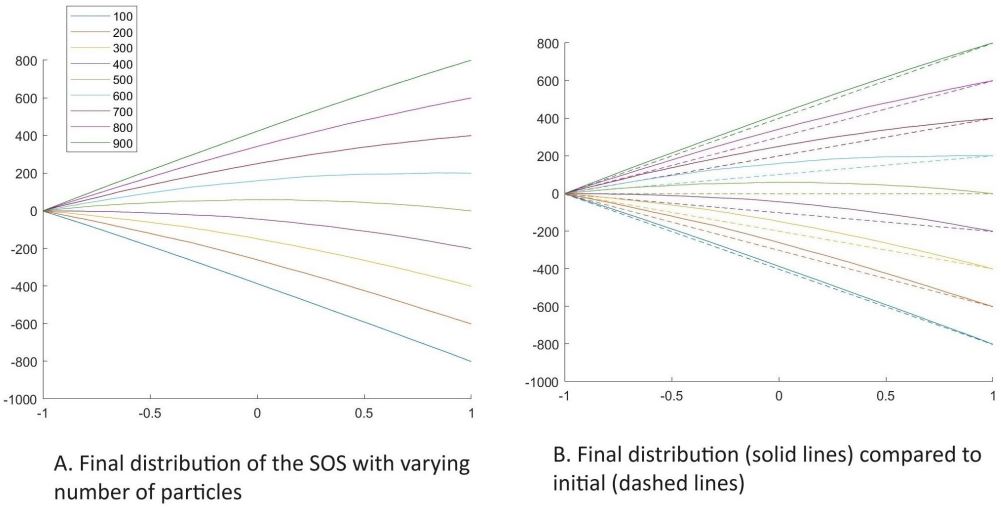

Figure 4.15: The SOS for a system with 1000 sites and different numbers of particles. Image A shows the final distribution of the SOS, and image B compares the final distribution to the initial for all systems.

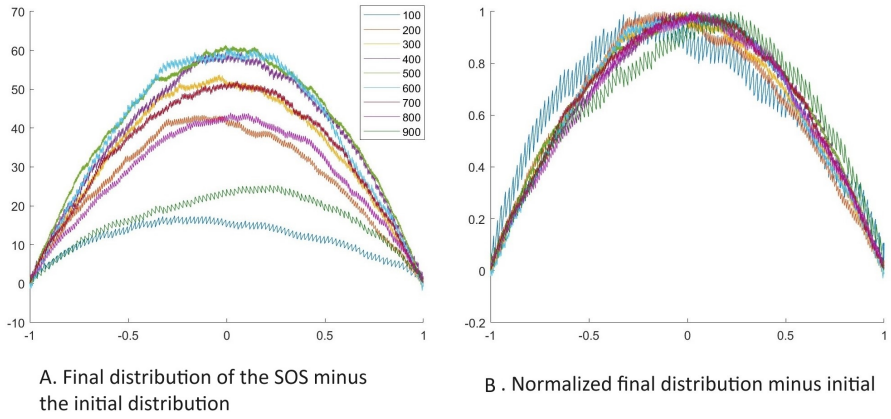

Figure 4.16: The same processes as in figure 4.15 but adjusted for initial conditions. Image A shows the final distribution minus the initial, and in image B the distributions are normalized.

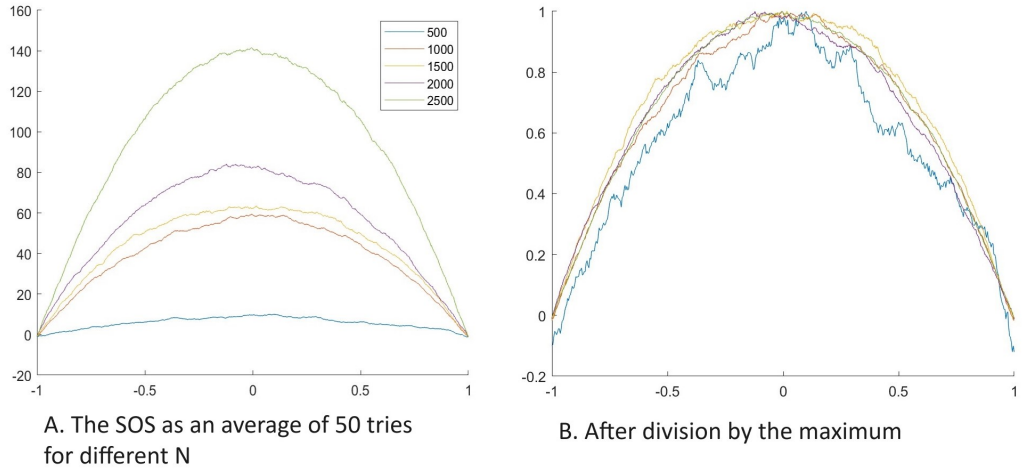

Figure 4.17: The average of 50 iterations of the SOS for a system where the initial distribution corresponds to every other site in the WASEP being occupied (i.e. the number of particles is $N/2$) for systems of different sizes. Image A shows the final distributions. In image B, these are normalized by dividing with the maximum value of the SOS.

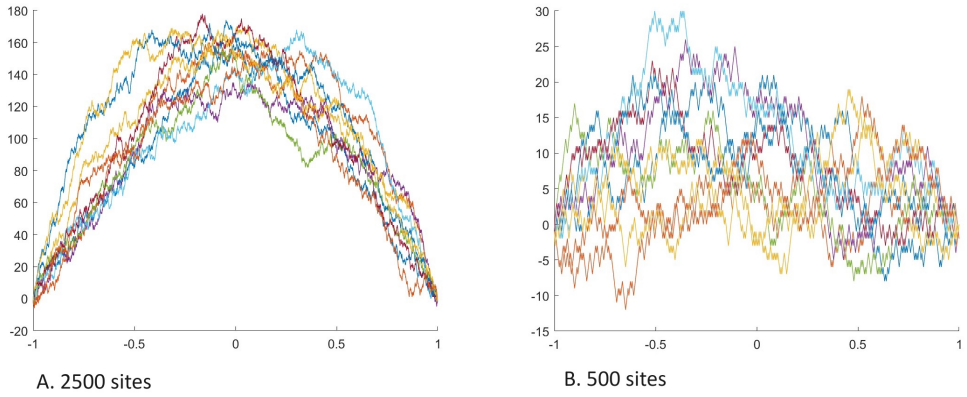

Figure 4.18: 10 instances of the SOS. The system has 2500 sites in A and 500 sites in B

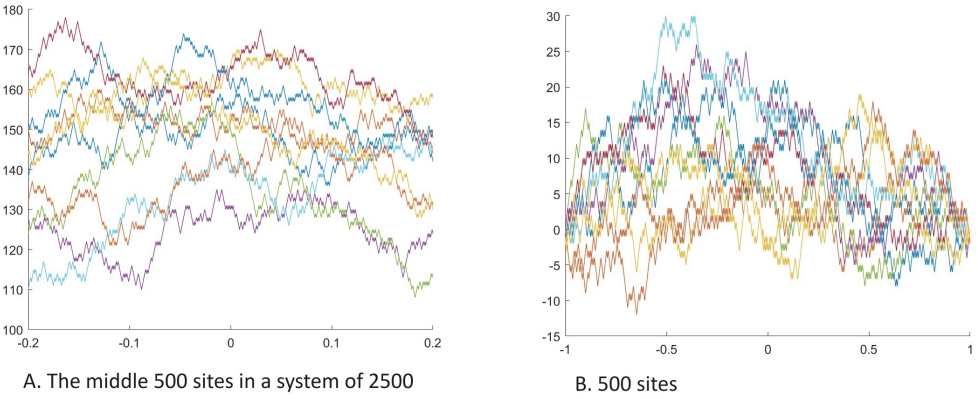

Figure 4.19: 10 instances of the SOS. A was simulated with 2500 sites and B with 500 and for both processes 500 sites are shown

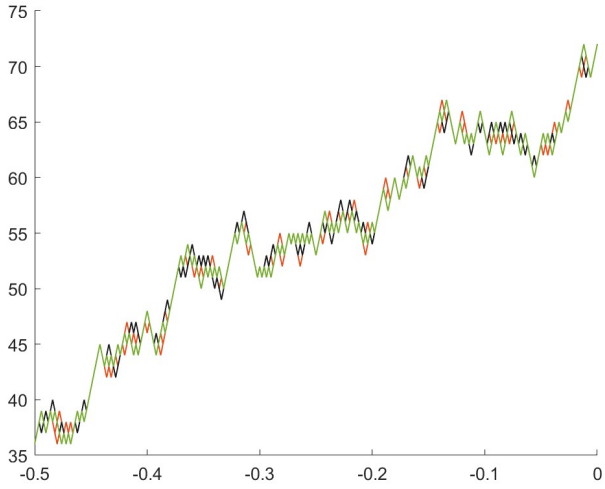

Figure 4.20: Zoomed in on one iteration of the SOS with 1000 sites and 500 particles. The initial configuration is in black and the final configuration 2.5s later is in green. The intermediary states are in orange

4.3.3 Conclusions

With a larger number of sites, both the SOS and WASEP become smoother and take longer to converge. The other main factor influencing the behaviour is the difference between empty and occupied sites in the WASEP. In the SOS, this difference is visible in the angle of the initial condition.

If the difference is low, convergence becomes faster, but the variance is higher. A SOS process with fixed end-points will grow to a parabola. If the initial distribution is close to horizontal, it becomes higher and smoother. The further from equal the number of occupied and empty sites is, the lower and rougher the parabola becomes, and the time it needs to converge becomes longer. Disregarding initial conditions, the behaviour of any two systems is similar if one has the same percentage of occupied sites that the other has empty.

Chapter 5

Scaling Limits

The results from the previous Chapter suggest that the average particle density of the WASEP and the mean height of the SOS approach stationary distributions as time and the number of sites increases. The individual particle systems fluctuate around the stationary average.

As the number of sites, N, increases on an interval, the discrete particle system model approaches a continuous model. The link between the discrete microscopic model described by a Markov generator and the macroscopic differential equation describing the large-scale behaviour of the system is, for an exclusion process, the hydrodynamic scaling limit. This scaling limit is obtained as N and t both approach infinity under appropriate scaling of time and space.

If space is scaled as $x = uN$ and the particle configuration of an exclusion process is denoted η_t, the associated empirical measure $\pi^N(\eta, du)$ is defined by

$$\pi^N(\eta, du) = \frac{1}{N} \sum_{\mathbb{T}_N} \eta_t(x) \delta_x(du), \tag{5.1}$$

where $\mathbb{T}_N = \mathbb{Z}/N\mathbb{Z}$ is the discrete torus with N sites. Assume that the initial configuration $\pi_0^N \to \rho_0(u)du$ in probability, with $\rho_0(u)$ being a smooth function on $\mathbb{T}_N$. Then, the empirical measure converges in distribution, i.e.

$$\{\pi_t^N, 0 \leq t \leq T\} \to \{\rho(t,u)du \; 0 \leq t \leq T\}, \tag{5.2}$$

where $\rho(t,u)$ is the unique solution to a partial differential equation

$$\partial_t \rho = \Delta h(\rho) \tag{5.3}$$

with initial condition $\rho(0,u) = \rho_0(u)$. The function h depending on the microscopic interaction. (Fra14)

Hydrodynamic limits can be applied for many particle systems, but there are also systems which do not converge (Fra14). The space in which the limits converge is $D\big([0,T], M_+\big)$, the space of right continuous functions with left limits taking values in the space $M_+(\mathbb{T})$ of finite positive measures on $\mathbb{T}$ with the weak topology.

Let Q^N be the probability measure on $D\big([0,T], M_+\big)$ which corresponds to the Markov process π_t^N, speeded up with N^2, and with initial distribution μ^N. There are several steps in the process to show that Q^N is a hydrodynamic limit to the system. First, the family Q^N has to be tight to guarantee convergence. The limit points must be concentrated on absolutely continuous trajectories that are weak solutions to the limiting PDE. This PDE should have a unique weak solution. Lastly, the empirical measure π^N needs to converge in probability to a deterministic measure $\pi_t(u)du$ (Lan02).

The set $\mathbb{T}_N$ contains the N sites of a realisation of an exclusion process with periodic boundaries. As $N \to \infty$, the space between particle sites will go to zero. Let η_t be a particle configuration for an exclusion process, π^N its associated empirical measure, and $G : \mathbb{T}_N \to \mathbb{R}$ a continuous function. Define

$$\langle \pi_t^N, G \rangle = \frac{1}{N} \sum_{x \in \mathbb{T}_N} G\left(\frac{x}{N}\right) \eta_t(x). \tag{5.4}$$

As N increases π^N approaches the continuous measure π and the sum $\langle \pi^N, G \rangle$ approaches the integral $\langle \pi, G \rangle = \int_{\mathbb{T}} G(u)\pi(du)$.

The Itô initial value problem

$$\begin{cases} d\xi(t) = f\big(\xi(t)\big)dt + g\big(\xi(t)\big)dW_t \\ \xi(0) = \xi_0 \end{cases} \tag{5.5}$$

is solved by the Itô process

$$\xi(T) = \xi(0) + \int_0^T f\big(\xi(t)\big)dt + \int_0^T g\big(\xi(t)\big)dW_t. \tag{5.6}$$

To find the limiting equation describing the equilibrium state of the process η_t, choose $\xi(t) = \langle \pi_t^N, G\rangle$, f as the Markov generator L_N for η, and g so that the martingale $\int_0^T \big(g(\xi(t)\big) dW_t$ vanishes in the limit. Inserting this into equation (5.6) yields

$$\langle \pi_t^N, G\rangle = \langle \pi_0^N, G\rangle + \int_0^T N^2 L_N \langle \pi_s^N, G\rangle ds + M_t^{G,N}. \tag{5.7}$$

There is a diffusive element in an exclusion process. Diffusion is described with the heat equation $\partial_t u = \partial_{xx} u$. In this equation, the first derivative of time corresponds to the second derivative of space. This suggests that for movement in an exclusion process to be noticeable, time must be scaled by ε^2 when space is scaled by ε. This is called the diffusive scaling, and the factor N^2 in front of the generator L_N originates from this.

5.1 Symmetric Simple Exclusion Process

As an example, consider the symmetric simple exclusion process. The Markov generator for the entire system using occupation variables $\eta(x) \in \{0, 1\}$ is

$$L_N f(\eta) = \frac{1}{2} \sum_x \Big(\eta(x)\big(1 - \eta(x+1)\big)\Big)\big[f(\eta^{x,x+1}) - f(\eta)\big] + \frac{1}{2} \sum_x \Big(\eta(x)\big(1 - \eta(x-1)\big)\Big)\big[f(\eta^{x,x-1}) - f(\eta)\big]. \tag{5.8}$$

For any one site x, the flow of particles leaving is

$$\frac{1}{2}\eta(x)\big(1 - \eta(x+1)\big) + \frac{1}{2}\eta(x)\big(1 - \eta(x-1)\big) \tag{5.9}$$

and the flow of arriving particles is

$$\frac{1}{2}\eta(x+1)\big(1 - \eta(x)\big) + \frac{1}{2}\eta(x-1)\big(1 - \eta(x)\big). \tag{5.10}$$

The total rate of change at site x will depend on

$$L_N \eta(x) = -\eta(x)\big(2 - \eta(x+1) - \eta(x-1)\big) + \big(1 - \eta(x)\big)\big(\eta(x+1) + \eta(x-1)\big), \tag{5.11}$$

which simplifies to

$$\frac{1}{2}\big(\eta(x+1)+\eta(x-1)-2\eta(x)\big)=\Delta\eta(x), \tag{5.12}$$

where Δ is the discrete Laplacian. Then

$$L_N\langle\pi_s^N,G\rangle=\frac{1}{2N}\sum_{x\in\mathbb{T}_N}G\left(\frac{x}{N}\right)\big[\eta(x+1)+\eta(x-1)-2\eta(x)\big]. \tag{5.13}$$

The sum in equation (5.13) is split into two parts, $\sum_{x\in\mathbb{T}_N}G\left(\frac{x}{N}\right)\big[\eta(x+1)-\eta(x)\big]$ and $\sum_{x\in\mathbb{T}_\mathbb{N}}G\left(\frac{x}{N}\right)\big[\eta(x-1)-\eta(x)\big]$. After summation by parts in equations (5.14) and (5.16) they are recombined in equation (5.17). The first part becomes

$$\begin{aligned}
&\sum_{x=1}^{N}G\left(\frac{x}{N}\right)\big(\eta(x+1)-\eta(x)\big)\\
=&G\left(\frac{N+1}{N}\right)\eta(N+1)-G\left(\frac{1}{N}\right)\eta(1)-\sum_{x=1}^{N}\eta(x+1)\left(G\left(\frac{x+1}{N}\right)-G\left(\frac{x}{N}\right)\right)\\
=&G\left(\frac{N+1}{N}\right)\eta(N+1)-G\left(\frac{1}{N}\right)\eta(1)-\sum_{x=0}^{N-1}\eta(x)\left(G\left(\frac{x}{N}\right)-G\left(\frac{x-1}{N}\right)\right).
\end{aligned} \tag{5.14}$$

Since the domain is a torus, $N+1$ refers to the same site as 1, and N and 0 are also equivalent. Thus $G\left(\frac{N+1}{N}\right)\eta(N+1)=G\left(\frac{1}{N}\right)\eta(1)$ and

$$\begin{aligned}
&\sum_{x=0}^{N-1}\eta(x)\left(G\left(\frac{x}{N}\right)-G\left(\frac{x-1}{N}\right)\right)\\
=&\sum_{x=1}^{N-1}\eta(x)\left(G\left(\frac{x}{N}\right)-G\left(\frac{x-1}{N}\right)\right)+\eta(N)G\left(\frac{N}{N}\right)-G\left(\frac{N-1}{N}\right)\Bigg)\\
=&\sum_{x=1}^{N}\eta(x)\left(G\left(\frac{x}{N}\right)-G\left(\frac{x-1}{N}\right)\right).
\end{aligned} \tag{5.15}$$

Similarly, the second part turns into

$$\begin{aligned}
&\sum_{\mathbb{T}_N} G\left(\frac{x}{N}\right)\left(\eta(x-1)-\eta(x)\right) \\
=&-G\left(\frac{N+1}{N}\right)\eta(N+1)+G\left(\frac{1}{N}\right)\eta(1)+\sum_{x=2}^{N+1}\eta(x)\left(G\left(\frac{x+1}{N}\right)-G\left(\frac{x}{N}\right)\right) \\
=&\sum_{x=1}^{N}\eta(x)\left(G\left(\frac{x+1}{N}\right)-G\left(\frac{x}{N}\right)\right).
\end{aligned} \tag{5.16}$$

They combine to

$$\sum_{x=1}^{N}\eta(x)\left(G\left(\frac{x+1}{N}\right)+G\left(\frac{x-1}{N}\right)-2G\left(\frac{x}{N}\right)\right)=\sum_{\mathbb{T}_N}\eta(x)\frac{1}{N^2}\Delta G\left(\frac{x}{N}\right), \tag{5.17}$$

transforming equation (5.7) into

$$\langle \pi_t^N, G\rangle = \langle \pi_0^N, G\rangle + \frac{1}{2}\int_0^t \left\langle \pi_s^N, \Delta G\left(\frac{x}{N}\right)\right\rangle + M_t^{G,N}, \tag{5.18}$$

where $M_t^{G,N}$ is a martingale.

Let Q^N be a probability measure corresponding to π^N speeded up by N^2 with initial condition μ_N. Q^N is relatively compact and will thus have a limit point. All limit points to Q^N at time 0 are concentrated on trajectories that are equal to $\rho_0(u)du$. Solving the martingale problem finds the limit points to Q^N at all times to be concentrated on absolutely continuous trajectories that are weak solutions of the stochastic heat equation with initial condition ρ_0. The weak solution to the stochastic heat equation is unique (Lan02). π_t^N converges in distribution to the deterministic measure $\pi_t(u)du$. This implies π_t^N converges in probability to a measure $\rho(u)$ which solves

$$\begin{cases} d_t\rho(t,u)=\frac{1}{2}\Delta\rho(t,u) \\ \rho(0,u)=\rho_0(u). \end{cases} \tag{5.19}$$

The detailed proof can be found in (Lan02).

5.2 Gradient systems

For more complicated particle systems, further assumptions are necessary to prove the uniqueness of the limit (Lan02). One such assumption for exclusion processes is for the system to be gradient. In this case, properties of the current facilitate calculations.

The current over $\{x, x+z\}$ is equal to the flow from x to $x+z$ minus the flow from $x+z$ to x. The generator $L_N\big(\eta(x)\big)$ can be described by the current of the process

$$L_N\eta(x) = W_{x-1,x} - W_{x,x+1} = -\nabla(W_{x,x+1}). \tag{5.20}$$

This relation gives a new expression for the part inside the integral in equation (5.7)

$$N^2 L_N\langle\pi, G\rangle = -\frac{1}{N}\sum_{\mathbb{T}_N} G\left(\frac{x}{N}\right)\nabla W_{x,x+1}. \tag{5.21}$$

Summing by parts yields

$$\begin{aligned} &-\frac{1}{N}\sum_{x=1}^{N-1} G\left(\frac{x}{N}\right)\nabla W_{x,x+1} \\ &= -\frac{1}{N}(G\left(\frac{N}{N}\right)W_{N-1,M} - G\left(\frac{1}{N}\right)W_{1,2} + \frac{1}{N}\sum_{x=1}^{N-1} W_{x,x+1}\nabla G\left(\frac{x}{N}\right). \end{aligned} \tag{5.22}$$

Because the state space is on a discrete torus, the endpoints have the same value and

$$N^2 L_N\langle\pi^N, G\rangle = \frac{1}{N}\sum_x (\nabla_N G)\left(\frac{x}{N}\right) N W_{x,x+1}, \tag{5.23}$$

where the discrete derivative is $\nabla_N = N\big(G(\frac{x+1}{N}) - G\left(\frac{x}{N}\right)\big)$.

If the current $W_{0,z}$ can be written as a sum of local functions h_n minus their translation $\tau_x h_n$ for every z it is called gradient (Lan02). The current of a gradient system is translation invariant; $W_{x,x+z} = \tau_x W_{0,z}$ for every x and z. The current $W_{x,x+1}$ can be written as a difference of the local functions and their translations $W_{x,x+1} = \tau_x \sum_{i=1}^{n_1}\{\tau_{x_{1,i}}h_{1,i} - h_{1,i}\}$. Inserting this into

equation (5.23), summation by parts is possible a second time. Equation (5.23) becomes

$$N^2 L_N \langle \pi^N, G \rangle = \frac{1}{N} \sum_x N \left\{ \nabla G \left(\frac{x}{N} \right) - \nabla G \left(\frac{x-1}{N} \right) \right\} \tau_x h, \tag{5.24}$$

which further simplifies to

$$N^2 L_N \langle \pi^N, G \rangle = \frac{1}{N} \sum_x G'' \left(\frac{x}{N} \right) \tau_x h\big(\eta(x)\big) + O(N^{-1}). \tag{5.25}$$

Since the martingale

$$M^N = \langle \pi_t^N, G \rangle - \langle \pi_0^N, G \rangle - \int_0^t N^2 L_N \langle \pi_s^N, G \rangle ds \tag{5.26}$$

vanishes at 0 its expectation is constantly 0 and

$$\mathbb{E}(\langle \pi_t^N \rangle - \langle \pi_0^N \rangle) = \mathbb{E}\Big(\int_0^t \sum_x G'' \left(\frac{x}{N} \right) \tau_x h\big(\eta(x) ds\big) + O(N^{-1}) \Big), \tag{5.27}$$

which converges to

$$\int_{\mathbb{T}_N} G(u)\rho(t,u)du - \int_{\mathbb{T}_N} G(u)\rho_0(t,u)du = \int_0^t \int_{\mathbb{T}N} G''(u) \mathbb{E}_{\mu_N} \Big[\tau_x h\big(\eta(x)\big) \Big] du ds. \tag{5.28}$$

The expectation $\mathbb{E}_{\mu_N}\big[\tau_x h\big(\eta(x)\big)\big] \sim E_{\nu^N_{\rho(s,x/N)}}[h]$ if local equilibria are conserved. Thus, if the empirical measure ρ converges, it must satisfy

$$\int_{\mathbb{T}_N} G(u)\rho(t,u)du - \int_{\mathbb{T}_N} G(u)\rho_0(t,u)du = \int_0^t \int_{\mathbb{T}_N} G''(u)\tilde{h}(\rho(s,u))du ds \tag{5.29}$$

for all smooth G and times t and $\tilde{h}(\rho(s,u)) = E_\rho[h] = \int h(\eta) d\rho(\eta)$. Therefore, ρ is a weak solution of the differential equation

$$\begin{cases} \partial_t \rho = \Delta \tilde{h}(\rho) \\ \rho(0) = \rho_0. \end{cases} \tag{5.30}$$

(Lan02)

5.3 Weakly Asymmetric Simple Exclusion Process

Though an exclusion process, the WASEP is not gradient. In this Section, the Markov generator for one site in the WASEP will be derived. The ideas in the proof of the convergence of the limit are discussed in Section (5.4).

From the Markov generator for the WASEP with $\eta \in \{0,1\}$

$$L_N f(\eta) = \frac{1}{2}\sum_x \Big(\eta(x)\big(1-\eta(x+1)\big)\Big)\Big[f(\eta^{x,x+1}) - f(\eta)\Big] + \Big(\frac{1}{2}+\sqrt{\varepsilon}\Big)\sum_x \Big(\eta(x)\big(1-\eta(x-1)\big)\Big)\Big[f(\eta^{x,x-1}) - f(\eta)\Big]. \quad (5.31)$$

The rate of change for one site x is found to be

$$L_N\eta(x) = -\frac{1}{2}\Big(\eta(x)\big(1-\eta(x+1)\big)\Big) - \Big(\frac{1}{2}+\sqrt{\varepsilon}\Big)\Big(\eta(x)\big(1-\eta(x-1)\big)\Big) + \Big(\frac{1}{2}+\sqrt{\varepsilon}\Big)\Big(\eta(x+1)\big(1-\eta(x)\big)\Big) + \frac{1}{2}\Big(\eta(x-1)\big(1-\eta(x)\big)\Big), \quad (5.32)$$

which simplifies into

$$L_N\eta(x) = \frac{1}{2}\Delta\eta(x) + \sqrt{\varepsilon}\Big(\eta(x+1)\big(1-\eta(x)\big) - \big(\eta(x)\big(1-\eta(x-1)\big)\Big) \quad (5.33)$$

and further to

$$L_N\eta(x) = \frac{1}{2}\Delta\eta(x) + \sqrt{\varepsilon}\Big(\nabla^+\eta(x) - \eta(x)\big(\nabla^+\eta(x) + \nabla^-\eta(x)\big)\Big) = \frac{1}{2}\Delta\eta(x) + \sqrt{\varepsilon}\big(\nabla\eta(x) + 2\eta(x)\nabla\eta(x)\big). \quad (5.34)$$

In the limit, the WASEP converges to the stochastic Burgers equation

$$\partial_t u_t = \frac{1}{2}\Delta u_t - \frac{1}{2}\nabla u_t^2 + \nabla\dot{W}_t. \quad (5.35)$$

The proof of convergence is analogous to the SOS and uses the relation $\eta_t(x) = \nabla^-\zeta(x)$.

5.4 Single Step Solid on Solid Process

The generator for the SOS (equation 3.9) in Section (3.2) has transition rates which depend on the local particle configuration. The transition rates are non-zero only when the criteria for a site being a local extreme point are met. The conditions determining the feasibility of transition need to be represented inside the Markov generator to derive the limiting equation for the SOS. To find a different expression for the generator, the SOS relationship to the WASEP is exploited. Let $\eta(x)$ be the configuration of the WASEP and set $\zeta_t(x) = \sum_{y \leq x} 2\eta(y) - 1$.

A particle moving one step to the right from site x to site $x+1$ in the WASEP corresponds to the local maximum between the relevant sites, becoming a local minimum in the SOS. This transition occurs at rate $\frac{1}{2}$ when the condition $\eta\big(x\big)\big(1-\eta(x+1)\big)$ is satisfied. A change from local minima to local maxima at the same position in the SOS transpires when a particle at site $x+1$ moves one step to the left. The transition rate for this is $\frac{1+\varepsilon}{2}$, and the condition to be satisfied is $\eta\big(x+1\big)\big(1-\eta(x)\big)$.

Putting this together leads to an expression of the generating function in the WASEP variables

$$L_N\eta(x) = -\frac{1}{2}\eta\big(x\big)\big(1-\eta(x+1)\big) + \left(\frac{1}{2}+\sqrt{\varepsilon}\right)\eta\big(x+1\big)\big(1-\eta(x)\big). \quad (5.36)$$

Simplifying, the symmetric part of the above equation becomes $\eta(x+1) - \eta(x)$. Using the relation $\zeta_t(x) = \sum_{y \leq x} 2\eta(y) - 1$ it can be expressed as $\frac{1}{2}\big(\zeta(x+1) - \zeta(x) + 1\big) - \frac{1}{2}\big(\zeta(x) - \zeta(x-1) + 1\big) = \frac{1}{2}\Delta\zeta(x)$.

The asymmetric part $\eta(x+1)\big(1-\eta(x)\big)$ translates to

$$\frac{1}{2}\Big(\zeta(x+1) - \zeta(x) + 1\Big)\Big(1 - \frac{1}{2}\big(\zeta(x) - \zeta(x-1) + 1\big)\Big), \quad (5.37)$$

which is equal to

$$\frac{1}{4}\big(1 + \nabla^+\zeta(x)\big)\big(1 - \nabla^-\zeta(x)\big). \quad (5.38)$$

Expanding yields

$$\frac{1}{4}\big(1+\nabla^+\zeta(x)-\nabla^-\zeta(x)-\nabla^+\zeta(x)\nabla^-\zeta(x)\big) \\ =\frac{1}{4}\big(\Delta\zeta(x)+1-\nabla^+\zeta(x)\nabla^-\zeta(x)\big). \quad (5.39)$$

The Markov generator for the SOS is found by combining the symmetric part, $\Delta\zeta(x)$, and the asymmetric part, in equation (5.39)

$$L_\varepsilon\zeta(x)=\Big(\frac{1}{2}+\sqrt{\varepsilon}\Big)\Delta\zeta(x)+\sqrt{\varepsilon}\big(1-\nabla^+\zeta(x)\nabla^-\zeta(x))\big). \quad (5.40)$$

With a diffusive scaling, it converges to the KPZ equation.(Ber96)

The Kardar-Parisi-Zhang equation (5.44) is proposed to describe the behaviour of the interface fluctuations in a random growth model. The growth of the interface height is characterised as a combination of diffusion, lateral growth and random forcing. To derive the model, the simplest non-trivial representation for these components is chosen as

$$\partial_t h_t=\nu\Delta h_t+F(\nabla h_t)+\sqrt{D}\xi_t. \quad (5.41)$$

Diffusion is represented by $\nu\Delta h_t$, with ν as the viscosity. The stochastic process ξ_t behind the random forcing is assumed to be independent in space and time and is modelled as white noise. The lateral growth ∇h_t depends on some function F. F is approximated by a Taylor expansion. The terms of third and higher order are irrelevant for large-scale behaviour. Inserting this expression in equation (5.41), it becomes

$$\partial_t h_t=\nu\Delta h_t+F(0)+F'(0)\nabla h_t+\frac{1}{2}F''(0)(\nabla h_t)^2+\sqrt{D}\xi_t. \quad (5.42)$$

$F(0)$ and $F'(0)t$ vanish with the Galilei transformation
$\tilde{h_t}(x)=h_t(x-F'(0)t)-F(0)t$. Set $F''(0)=\lambda$. With these choices for the noise and lateral growth, equation (5.42) becomes the KPZ equation

$$\partial_t\tilde{h_t}=\nu\Delta\tilde{h_t}+\frac{1}{2}\lambda(\nabla\tilde{h_t})^2+\sqrt{D}\dot{W}_t. \quad (5.43)$$

Choose the parameters $\nu=\frac{1}{2}$, $\lambda=-1$ and $D=1$ and set $h=\tilde{h}$. (Kru92)(Qua11)
The previous equation becomes

$$\partial_t h_t=\frac{1}{2}\Delta h_t-\frac{1}{2}(\nabla h_t)^2+\dot{W}_t. \quad (5.44)$$

The function $h_t(x)$ is the height at x, or the distance from a starting line to the interface. Locally, on a small scale, the behaviour of h_t depends on all three terms on the right-hand side of the equation (5.44). However, it is assumed that when moving to a coarser scale by grouping particles together, the only relevant term is Δh_t.

The Wiener Process has covariance $\mathrm{E}\big(W_t(r), W_s(r)\big) = (t \wedge s)$. Define the mollified Wiener process $W_t^\kappa(r) = W_t(\delta_r^\kappa)$, where $\delta_r^\kappa(r) = \kappa J\big(\kappa(r-r)\big)$ for an even positive function $J \in C_0^\infty(\mathbb{R})$ where $\int J dr = 1$. This process has a covariance resembling a tent function: $\mathrm{E}\big(W_t^\kappa(r), W_s^\kappa(r)\big) = (t \wedge s)(\delta_{r-r}^\kappa, \delta_0^\kappa)$. Replacing W_t in equation (5.44) by W_t^κ will avoid difficulties when integrating infinitely many W_t. As $\delta^\kappa \to \delta$ when $\kappa \to 0$, W_t^κ converges to W_t. Rewriting the KPZ equation (5.44) into integral form with test functions and W_t^κ gives

$$\int_0^t \partial(h_s^\kappa, \phi) ds = \int_0^t \big\{\frac{1}{2}\Delta(h_s^\kappa, \phi) - \frac{1}{2}\big(\nabla(h_s^\kappa, \phi)\big)^2\big\} ds + \int_0^t (\dot{W}_s^\kappa, \phi) ds. \quad (5.45)$$

Integrating by parts and adding the Wick product of the non-linearity gives

$$h_t^\kappa(\phi) = h_0(\phi) + \frac{1}{2}\int_0^t \Big\{h_s^\kappa(\phi'') - \big[(\nabla h_s^\kappa)^2 - C_\kappa(0)\big](\phi)\Big\} ds + W_t^\kappa(\phi). \quad (5.46)$$

The Wick product, $C_\kappa(0) \sim \frac{1}{\kappa}$, originates from the extra term in the Itô integral. The initial condition h_0 is assumed to be continuous, and for every $r \in \mathbb{R}$ the exponential moment $\mathrm{E}\big(e^{p \cdot h_0(r)}\big)$ can grow at most exponentially in r. Since W_t^κ is smooth for finite κ, equation (5.46) can be solved by a differentiable process $h^\kappa \in C\big([0,T]; C\big(\mathbb{R}\big)\big) \cap C\big((0,T]; C^1(\mathbb{R})\big)$. The family $\{h^\kappa\}_{\kappa>0}$ converges weakly as $\kappa \to \infty$ in the topology of $C([0,T]; C\big(\mathbb{R}\big))$.

The function $\bar{\zeta}$ is defined in Section 3.2 as the linear interpolation of the SOS process. Scaling in time and space and adding the Wick term $\nu_\varepsilon t = \frac{1}{2}\varepsilon^{-\frac{3}{2}} - \frac{1}{24}\varepsilon^{-\frac{1}{2}}$ yields $Z_t^\varepsilon(r) = \sqrt{\varepsilon}\big(\bar{\zeta}_{\varepsilon^{-2}t}(\varepsilon^{-1}r) - \nu_\varepsilon t\big)$. When the initial distribution has the right properties the family $\{Z^\varepsilon\}_{\varepsilon>0}$ converges weakly as $\varepsilon \to 0$.

$\{h^\kappa\}_{\kappa>0}$ and $\{Z^\varepsilon\}_{\varepsilon>0}$ converge to the same process.

To prove this, Bertini and Giacomin apply a transformation to the KPZ equation and a microscopic analogue to this transformation on the fluctuation field and show that they both converge to a solution of the stochastic

heat equation (Ber97).

The linear interpolation of a valid initial distribution of the SOS converges in the right scaling to a random function that satisfies the conditions for an initial function of the KPZ equation. Assume $\bar{\zeta}$ to be a continuous function by linear interpolation, scale this interpolated function as $\bar{\zeta}^\varepsilon = \sqrt{\varepsilon}\,\bar{\zeta}\big(\frac{1}{\varepsilon}r\big)$ and let ζ_0 fulfil the conditions for an initial distribution of the SOS. Then there exists a random function $h_0 \in C(\mathbb{R})$ such that $\bar{\zeta}^\varepsilon$ converges weakly to h_0 in the topology of $C(\mathbb{R})$ as $\varepsilon \to 0$.

The function h_0 defined as above will be Hölder continuous with exponent less than $\frac{1}{2}$. This process is continuous but not differentiable, and behaves like a random walk. h_0 satisfies the conditions for an initial function for the KPZ equation (5.44)(Ber97).

Using the Cole-Hopf transformation $\theta_t = e^{-h_t}$ on equation (5.44), it becomes the stochastic heat equation

$$d\theta_t = \frac{1}{2}\Delta\theta_t dt - \theta_t dW_t. \tag{5.47}$$

For a bounded interval on $\mathbb{R}$, the existence and uniqueness of the solution to equation (5.47) are already proved. Define $\Psi : D\big([0,T]; C(\mathbb{R})\big) \mapsto D\big([0,T] : C(\mathbb{R})\big)$ as

$$\Psi(f_t(r)) = \begin{cases} -\log f_t(r) & \text{if} \quad f \in D\big([0,T]; C_+(\mathbb{R})\big), \\ 0 & \text{otherwise.} \end{cases} \tag{5.48}$$

If θ is a solution to the stochastic heat equation, and $\theta \in C_+(\mathbb{R})$, $\Psi(\theta) = h$ is a solution to the KPZ equation. (Thm 3.1 and 3.2 in (Ber97)).

The transformation for the fluctuation field corresponding to Cole-Hopf is the Gärtner transformation

$$\xi_t(r) = \exp\{-\gamma_\varepsilon \bar{\zeta}_t(r) + \lambda_\varepsilon t\} \tag{5.49}$$

where $\gamma_\varepsilon = \frac{1}{2}\log(1 + 2\sqrt{\varepsilon})$ and $\lambda_\varepsilon = 1 + \sqrt{\varepsilon} - \sqrt{1 + 2\sqrt{\varepsilon}}$. Using the inverse map to the Gärtner transform, Z_t^ε can be rewritten as

$$Z_t^\varepsilon(r) = -\frac{\sqrt{\varepsilon}}{\gamma_\varepsilon}\log\big(\xi_t^\varepsilon(r)\big) + \sqrt{\varepsilon}\left[\frac{\lambda_\varepsilon}{\gamma_\varepsilon}\varepsilon^{-2} - \nu_\varepsilon\right]t. \tag{5.50}$$

Since $\lim_{\varepsilon\to 0}\frac{\sqrt{\varepsilon}}{\gamma_\varepsilon} = \frac{\sqrt{\varepsilon}}{\frac{1}{2}(1+2\sqrt{\varepsilon})} = 1$ and there exists a constant c such that $|\frac{\lambda_\varepsilon}{\gamma_\varepsilon}\varepsilon^{-2} - \nu_\varepsilon| \leq c$ for all $\varepsilon \in (0,1)$ most variables disappear from Z^ε as $\varepsilon \to 0$. For ε close to 0 equation (5.50) simplifies to

$$Z_t^\varepsilon(r) = -\log\big(\xi_t^\varepsilon(r)\big) = \Psi\big(\xi_t^\varepsilon(r)\big). \tag{5.51}$$

When ξ is scaled diffusively as $\xi_t^\varepsilon(r) = \xi_{\varepsilon^{-2}t}(\varepsilon^{-1}r)$ the family $\{\xi_t^\varepsilon\}_{\varepsilon>0}$ converges weakly to θ as $\varepsilon \to 0$, where θ is the solution to the stochastic heat equation. The proof can be found in (Ber97). It is done by identifying the limit through formulating the martingale problem for the stochastic heat equation and proving that the family $\{\xi^\varepsilon\}_{\varepsilon>0}$ converges to a process ξ with the same law as the unique solution to this problem.

ξ^ε converges to the solution of the stochastic heat equation (5.47), and therefore Z^ε converges to h, which is the solution to the KPZ equation (5.44). Thus, the solution of the KPZ equation can be derived as the scaling limit of the SOS particle system.

5.5 KPZ Universality

The KPZ equation was invented to describe a growth process whose evolution depends on both a smoothing, diffusive part and a growth rate, where the growth rate is a combination of a non-linear dependence of growth rate on the local slope and space-time independent noise. This is true for the SOS and for various other models which are said to belong to the KPZ universality class. It is predicted that for all these models at the time t, the fluctuations around the mean will be on the scale $t^{\frac{1}{3}}$, and the process will be spatially correlated on a $t^{\frac{2}{3}}$ scale. Experiments have confirmed this behaviour in several cases, such as liquid crystal growth and bacterial colony growth (Cor16), (Rem22).

There is not yet a concrete definition of which models belong to the KPZ universality class. Aside from the SOS, other models in the class include directed polymers and ballistic growth processes. Much of the research on KPZ universality has been done with the TASEP since it has the specific properties necessary for the Gärtner transform.(Bai22), (Cor11).

The KPZ universality conjecture states that for any model in this class, the associated height function h should, with scaling, converge to the same process

$$\lim_{\varepsilon \to 0} \varepsilon^{\frac{1}{2}} \left(h(c_1 \varepsilon^{-\frac{3}{2}} t, c_2 \varepsilon^{-1} x) - c_3 \varepsilon^{\frac{3}{2}} t \right) = \mathfrak{h} \tag{5.52}$$

where $\mathfrak{h}$ depends only on the initial condition $\mathfrak{h}_0 = \lim_{\varepsilon \to 0} \varepsilon^{\frac{1}{2}} h(0, c_2 \varepsilon^{-1} x)$. $\mathfrak{h}$ is called the KPZ fixed point. It is expected to be a Markov process and is invariant under the $1:2:3$ scaling (Rem22)

$$\mathfrak{h}(x,t) = \alpha \mathfrak{h}(\alpha^{-2} x, \alpha^{-3} t) \tag{5.53}$$

Chapter 6

Current state of research and open problems

To show convergence in the scaling limit to the KPZ equation, Bertini and Giacomin (Ber97) use a method based on the linearisation of both the particle system model and the partial differential equation. This relies on the linearised differential equation to be well-defined and for the microscopic transform of the particle system to give a meaningful result. The WASEP has specific properties that make this approach work, but for most models, it does not.

To circumvent this restriction Gonçalves and Jara (Gon14) and Hairer (Hai12) propose new forms of solutions to the KPZ equation, and Flandoli et al (Fla21) and Dembo and Tsai (Dem16) find ways to link other models to the TASEP and utilise that connection to prove the scaling limit of the other models. The methods for investigating the KPZ equation in 1 space dimension fail for $d \geq 2$ when the stochastic heat equation is no longer well-defined. Chatterjee (Cha22) and Tao (Tao23) investigate scaling limits in multiple dimensions.

(Gon14) introduces the notion of energy solutions of stochastic differential equations, which gives a well-defined solution of the KPZ equation without relying on the Cole-Hopf transform and the stochastic heat equation. The idea behind energy solutions is to regularise the non-linear term with noise in the time variable. This method works for particle systems without the properties of the WASEP. The energy solution of the KPZ is the same as the

solution obtained by using the Cole-Hopf transform. A process is considered an energy solution if two criteria limiting expectations and norms hold, and it is a martingale fulfilling a specific equation (Gon14).

In (Hai12), Hairer introduces a new concept of solution to the KPZ equation that builds on writing the solution as a Wild expansion whose components are related to the solution to the stochastic heat equation. The series is truncated, the parts in the series are proved convergent, and the residual is shown to be a solution to a solvable equation. This construction of a solution avoids the Cole-Hopf transform and enables analysis of a broader range of problems. (Hai12).

Because of the non-uniqueness of weak solutions, the solution of a deterministic differential equation with deterministic initial condition can be a stochastic process (Fla21). Flandolini et al (Fla21) consider a class of weak solutions to the Burgers equation where the second and third derivative goes to zero and whose characterisation is unknown. By finding a bijection, they link these to a particle system model called the Active Bi-Directional Flow and the TASEP, thus showing that the TASEP can be interpreted as a stochastic weak solution to the deterministic Burgers equation.

In a non-simple exclusion process, particles can jump to sites that are not their neighbours. These processes also converge to the KPZ equation, which was proven in (Dem16) for jumps of length 3 or smaller and in (Yan23) for jumps of finite arbitrary length. It is an analytic method that compares the transition probabilities of any asymmetric exclusion process with finite length to the TASEP and finds they have the same scaling limit and, thus, belong to the KPZ universality class.

There are many models where the scaling of fluctuations and spatial correlation imply they belong to the KPZ universality class, where rigorous analysis of the scaling limit is impossible. There is not yet a concrete definition of which models belong in the KPZ universality class. If there is an explicit construction of the KPZ fixed point, the universality conjecture (5.52) can be used to formulate a concrete definition of the KPZ universality class. (Rem22).

For dimension $d > 1$, the stochastic heat equation ceases to be well-posed.

Using the correct scaling in two dimensions, the height function for particles sufficiently close to each other converges in joint distribution to the multi-dimensional normal distribution. The local average of h_ε, the solution to a 2d KPZ driven by mollified space-time white noise on a ball, converges to a sum of a Gaussian process, a constant and the solution to the deterministic KPZ equation (Tao23).

In higher dimensions, there is no known method of how to take non-trivial scaling limits, and even in one dimension, there can be many scaling limits to the same model. Instead, in (Cha22), Chatterjee shows that there is a general class of growth models for which the scaling limit, regardless of how it is taken, locally behaves like a KPZ equation. For these models, the limiting function can be decomposed into a Laplacian term, a gradient squared term, a noise term and a negligible residual.

Bibliography

[Bar22] Barraquand G, Krajenbrink A, Le Doussal P. (2022) *Half-space stationary Kardar–Parisi–Zhang equation beyond the Brownian case.* J.Phys.A:Math.Theor. 55 275004. https://arxiv.org/abs/2202.10487

[Bai22] Baik J. (2022) *KPZ limit theorems.* A survey paper for ICM 2022 proceedings. https://arxiv.org/pdf/2206.14086.pdf

[Ber97] Bertini L, Giacomin G. (1997). *Stochastic Burgers and KPZ equations from Particle Systems.* Communications in Mathematical Physics 183, p571 - 607. https://link.springer.com/article/10.1007/s002200050044

[Ber96] Bertini L (1996) *Microscopic derivation of Kardar-Parisi-Zhang Equation.* https://arxiv.org/abs/cond-mat/9601067

[Brz99] Brzeźniak Z, Zastawniak T (1999) *Basic Stochastic Processes.* Springer-Verlag London

[Cal83] Calderoni P, Pulvirenti M. (1983) *Propagation of chaos for Burgers' equation.* Annales de l'I. H. P., Section A, tome 39, no 1 (1983), p. 85-97. www.numdam.org/article/AIHPA_1983__39_1_85_0.pdf

[Cha21] Chatterjee S. (2021) *Universality of deterministic KPZ.* https://arxiv.org/abs/2102.13131

[Cha22] Chatterjee S. (2022) *Local KPZ Behavior under Arbitrary Scaling Limits.* Commun. Math. Phys. 396, 1277–1304 (2022). https://arxiv.org/abs/2110.01062

[Cor11] Corwin I. (2011) *The Kardar-Parisi-Zhang equation and universality class*. Random Matrices: Theory and Applications Vol.01, No 01, 1130001. https://arxiv.org/abs/1106.1596

[Cor16] Corwin I. (2016) *Kardar-Parisi-Zhang universality*. Notices Amer. Math. Soc., 63 no. 3, 230–239. https://arxiv.org/abs/1606.06602

[Dun21] Dunlap A, Graham C, Ryzhik L. (2021) *Stationary solutions to the stochastic Burgers equation on the line*. Communications in Mathematical Physics, 382(2), 875–949. https://arxiv.org/abs/1910.07464

[Dem16] Dembo A, Tsai L. (2016) *Weakly Asymmetric Non-Simple Exclusion Process and the Kardar-Parisi-Zhang Equation*. Commun. Math. Phys. 341, 219–261. https://arxiv.org/abs/1302.5760

[Fay11] Fayolle G, Furtlehner C. (2011) *About Hydrodynamic Limit of Some Exclusion Processes via Functional Integration*. International Mathematical Conference "50 YEARS OF IITP", Institute for Information Transmission Problems (Russian Academy of Sciences), Jul 2011, Moscow, Russia. https://arxiv.org/abs/1201.5185

[Fla21] Flandoli F, Gess B, Grotto F. (2021) *An Example of Intrinsic Randomness in Deterministic PDES*. Stochastics and Dynamics. Vol. 22, No. 07, 2240023. https://arxiv.org/abs/2012.04398

[Fra14] Franco T. (2014) *Interacting particle systems: hydrodynamic limit versus high density limit*. From Particle Systems to Partial Differential Equations. Springer Proceedings in Mathematics Statistics Volume 75, 2014, pp. 179-189 https://arxiv.org/abs/1401.3622

[Fra13] Franco T, Gonçalves P, Neumann A. (2013) *Slowed exclusion process: hydrodynamics, fluctuations and phase transitions*. From Particle Systems to Partial Differential Equations. Springer Proceedings in Mathematics Statistics Volume 75, 2014, pp. 191-205. https://arxiv.org/abs/1310.5161

[Gon07] Gonçalves P. (2007) *Central Limit Theorem for a Tagged Particle in Asymmetric Simple Exclusion*. Stochastic Processes and their

Applications, Vol. 118, 474 - 502. https://arxiv.org/abs/math/0611505

[Gon14] Gonçalves P, Jara M. (2014) *Nonlinear Fluctuations of Weakly Asymmetric Interacting Particle Systems.* Arch. Rational Mech. Anal. 212 597–644. https://arxiv.org/abs/1309.5120

[Hai12] Hairer M. (2012) *Solving the KPZ equation.* Annals of Mathematics 178 (2013), 559–664. https://arxiv.org/abs/1109.6811

[Hay22] Hayashi K. (2022) *Equilibrium Fluctuations for Totally Asymmetric Interacting Particle Systems.* Online Young Summer Seminar on Probability Theory, August 2021. https://arxiv.org/abs/2201.01987

[Kel12] Kelling J, Ódor G. (2012) *Extremely large scale simulation of a Kardar-Parisi-Zhang model using graphics cards.* Phys Rev E Stat Nonlin Soft Matter Phys. 2011 Dec;84(6 Pt 1):061150. doi: 10.1103/PhysRevE.84.061150. Epub 2011 Dec 28. Erratum in: Phys Rev E Stat Nonlin Soft Matter Phys. 2012 Jan;85(1 Pt 2):019902. PMID: 22304083. https://arxiv.org/abs/1110.6745

[Kru92] Krug J, Spohn H. (1992) *Kinetic roughening of growing interfaces.* Solids Far from Equilibrium: Growth, Morphology and Defects, pages 479–582. Cambridge University Press, Boston, MA. https://www.thp.uni-koeln.de/krug/publikationen-Dateien/KrugSpohn.pdf

[Jar05] Jara M.D, Landim C. (2005) *Nonequilibrium Central Limit Theorem for a Tagged Particle in Symmetric Simple Exclusion.* Annales de l'I.H.P. Probabilités et statistiques, Volume 42 (2006) no. 5, pp. 567-577. http://www.numdam.org/item/10.1016/j.anihpb.2005.04.007.pdf

[Lan02] Landim C. (2002) *Hydrodynamic Limit of Interacting Particle Systems.* Lectures given at the School and Conference on Probability Theory Trieste, 13-31 May 2002. https://www.osti.gov/etdeweb/servlets/purl/20945055

[Lig85] Liggett T. (1985). *Interacting Particle Systems.* Reprint: Springer Berlin Heidelberg, Classics in mathematics, 2005.

[Qua11] Quastel J. (2011) *Introduction to KPZ*. Current Developments in Mathematics 1 2011. https://www.math.toronto.edu/quastel/survey.pdf

[Qua21] Quastel J, Sarkar S. (2021) *Convergence of exclusion processes and the KPZ equation to the KPZ fixed point*. J. Amer. Math. Soc. 36 (2023), 251-289. https://arxiv.org/abs/2008.06584

[Ram23] Ramanan K. (2023) *Interacting stochastic processes on sparse random graphs*. Invited Paper, Proceedings of the 2022 ICM, Vol. 6, pp. 4394–4425. https://arxiv.org/abs/2401.00082

[Rem22] Remenik D. (2022) *Integrable fluctuations in the KPZ universality class*. Proceedings of the ICM 2022, Vol. 6, 4426-4450 (2023) https://arxiv.org/abs/2205.01433

[Sac76] Sachdev P.L. (1976) *Some Exact Solutions of Burgers-Type Equations*. Quarterly of Applied Mathematics, April 1976, pages 118-122. https://www.jstor.org/stable/43636797

[She18] Shen H, Weber H. (2018) *Glauber dynamics of 2D Kac-Blume-Capel model and their stochastic PDE limits*. Journal of Functional Analysis Volume 275, Issue 6, 15 September 2018, Pages 1321-1367. https://arxiv.org/abs/1608.06556

[Tao23] Tao R. (2023) *Mesoscopic Averaging of the Two-Dimensional KPZ Equation*. Journal of Statistical Physics (2024) 191:6. https://arxiv.org/abs/2302.06689

[Var90] Varadhan S.R.S. (1990) *Scaling Limits for Interacting Diffusions*. Commun. Math. Phys. 135, 313-353 (1991). https://projecteuclid.org/journals/communications-in-mathematical-physics/volume-135/issue-2/Scaling-limits-for-interacting-diffusions/cmp/1104202029.pdf

[Yan23] Yang K. (2023) *Kardar–Parisi–Zhang Equation from Long-Range Exclusion Processes*. Commun. Math. Phys. 400, 1535–1663. https://arxiv.org/abs/2002.05176

[Zha22] Zhang L. (2022) *Cutoff profile of the Metropolis biased card shuffling*. https://arxiv.org/abs/2208.13383

Appendix A

Definitions

A.1 σ-fields and filtrations

In statistics, knowledge of possible events is represented by σ-fields. A **σ-field** $\mathcal{F}$ is defined as a family of subsets on a non-empty set Ω such that (1) $\emptyset \in \mathcal{F}$, (2) both the set A and its complement $\Omega \backslash A$ are in $\mathcal{F}$ and (3) the union of any sequence of sets in $\mathcal{F}$ is also in $\mathcal{F}$. The sets in $\mathcal{F}$ are called events.

A **filtration** is a sequence of σ-fields on Ω such that $\mathcal{F}_1 \subset \mathcal{F}_2 \subset \ldots \subset \mathcal{F}$. The σ-field $\mathcal{F}_n$ represents our knowledge at time n and contains all events for which it is possible to discern whether or not they have occurred.

A.2 Random variables

A random variable is defined as a $\mathcal{F}$-measurable function $\xi : \Omega \mapsto \mathbb{R}$. A function is **measurable** if it can be known, i.e. $\{\omega \in \Omega : \xi(\omega) \in B\} \in \mathcal{F}$ for all Borel sets $B \in \mathbb{R}$) with a Borel set being the smallest σ-field to contain all intervals in $\mathbb{R}$. A sequence of random variables is **adapted to a filtration** if ξ_n is $\mathcal{F}_n$-measurable, i.e. $\xi_n \in \mathcal{F}_n$ for all n.

A probability measure $\mathrm{P} : \mathcal{F} \mapsto [0,1]$ is a function with the properties $\mathrm{P}(\Omega) = 1$ and if $A_1, A_2, \ldots$ are disjoint sets $\mathrm{P}(A_1 \cup A_2 \cup \ldots) = \mathrm{P}(A_1) + \mathrm{P}(A_2) + \ldots$. Together, $(\Omega, \mathcal{F}, \mathrm{P})$ make up a probability space.

Integrable random variables, expectation and variance Integrable in the case of random variables refers to the Lebegue integral with respect to a probability measure P. The random variable ξ is integrable if $\int_\Omega |\xi| d\mathrm{P} < \infty$, and the expectation is then defined as $\mathrm{E}(\xi) = \int_\Omega \xi d\mathrm{P}$. If $\int_\Omega |\xi|^2 d\mathrm{P} < \infty$ ξ is square integrable. If a random variable is square integrable its variance is $\int_\Omega (\xi - \mathrm{E}(\xi))^2 d\mathrm{P}$

Conditional Expectation The conditional expectation $\mathrm{E}(\xi|\mathcal{G})$ for the random variable ξ given a σ-field $\mathcal{G} \subset \mathcal{F}$ is a random variable which is $\mathcal{G}$ measurable, and for which all events $A \in \mathcal{G}$ the expectation $\int_A \mathrm{E}(\xi|\mathcal{G}) d\mathrm{P} = \int_A \xi d\mathrm{P}$. The conditional expectation has the following properties

1. $\mathrm{E}(\alpha\xi + \beta\zeta|\mathcal{G}) = \alpha\mathrm{E}(\xi|\mathcal{G}) + \beta\mathrm{E}(\zeta|\mathcal{G})$
2. $\mathrm{E}(\mathrm{E}(\xi|\mathcal{G})) = \mathrm{E}(\xi))$
3. $\mathrm{E}(\xi\zeta|\mathcal{G}) = \xi\mathrm{E}(\zeta|\mathcal{G})$ if ξ is $\mathcal{G}$-measurable.
4. $\mathrm{E}(\xi|\mathcal{G}) = \mathrm{E}(\xi)$ is ξ is independent of $\mathcal{G}$
5. $\mathrm{E}(\mathrm{E}(\xi|\mathcal{G})|\mathcal{H}) = \mathrm{E}(\xi|\mathcal{H})$ if $\mathcal{H} \subset \mathcal{G}$.
6. If $\xi \geq 0$ then $\mathrm{E}(\xi|\mathcal{G}) \geq 0$

(Brz99)

A.3 Stochastic Processes

A family of random variables $\xi(t)$ parametrized by $t \in T$ is called a **stochastic process**. For every $\omega \in \Omega$ the function $t \to \xi(t, \omega)$ is called a **path** or **sample path** of $\xi(t)$.

Appendix B

Code

B.1 MATLAB

For simulations of the long-time distribution of particles in the WASEP

```
%WASEP, impassable borders, vary occupancy and epsilon
k = 50; %nbr of iterations
xMax = 1000; %nbr of positions
tMax = xMax;
kTagged = zeros(k,tMax);
kWASEPprev =zeros(k,xMax); %latest configuration
kWASEPsave = zeros(k,41,xMax); %save at certain
intervals
xInit = repmat([0,1], 1, 500); %flat, 500 particles
epsilon = 1/xMax; %the asymmetry is the inverse of the
                  space scaling
saveInd = 1;

Q = (1 + (epsilon))/2; %left intensity
P = 1/2; %right intensity
q = Q/(Q + P); %normalize left
p = P/(Q + P); %normalize right

for ind = 1:k %initialize for all k simulations
    kWASEPprev(ind,:) = xInit;
```

```
    kWASEPsave(ind,1,:) = xInit;
end


for tInd = 1:4*tMax
    kWASEPtInd = zeros(ind,xMax); %temporary
for ind = 1:k
    tInd %print out which for loop is active
    ind  %to estimate the time until the simulation
          finishes

%Initialize

A = zeros(tMax*xMax/4, 3); %allocate space for poisson
                            processes for all sites.
tagged = find(xWASEP > 0, 1); %the tagged particle is
                               the leftmost one

tagged_left = tagged; %keep track of the leftmost
                       position of the tagged particle
tagged_right = tagged; %-"- rightmost
tagged_init = tagged; %initial position for this
                        simulation

%initialize jumps

time = 0; %time at the start of a Poisson process
index = 1; % index of the first non-occupied row of A
for pos = 1:xMax %generate a Poisson process with
                  intensity (2 + epsilon)/2
    U = rand(tMax,1);
    X = -log(1 - U)/(P + Q); %exponentially distributed
                              variables
    T_all = cumsum(X); %a Poisson process
    ind_T = find(T_all > tMax/4, 1);
    T = T_all(1: ind_T - 1); %the non-zero elements
    n_T = length(T);
```

```
    p_dir = rand(n_T, 1);
    p_left = p_dir \langle q; % p(left) = q
    dir = ones(n_T, 1);
    dir = dir - 2*p_left; %dir = 1 if right, -1 if left
    J = [T, pos*ones(n_T,1), dir]; %the Poisson process
                                    at site pos.
                                    Stores time,
                                    position before jump
                                    and jump direction

   A(index:index + n_T - 1,:) = J;
   index = index + n_T;

end

temp = A(any(A,2),:); %delete redundant (zero) rows of A
A = sortrows(temp,1); %sort by time

[m,n] = size(A);

%step
for t = 2:m %all jumps in A
     j = A(t,:);
     from = j(2);
     direction = j(3);
     to = from + direction;

      if to > xMax || to \langle 1
         %nothing happens, the borders are impassable
     else %interior movement

         if xWASEP(from) == 1 && xWASEP(to) == 0
         %movement only if from occupied and to empty

             xWASEP(from) = 0;
             xWASEP(to) = 1;
             if tagged == from
                 tagged = to;
```

```
                if (to > tagged_right)
                    tagged_right = to;
                elseif (to \langle tagged_left)
                    tagged_left = to;
                end
            end
        end
    end

    kTagged(ind, tInd, 1) = tagged_left;
    kTagged(ind,tInd,2) = tagged_right;
    kTagged(ind,tInd,3) = tagged_init;
    kWASEPtInd(ind,:) = xWASEP;

    kWASEPprev = kWASEPtInd; %last configuration will be
                             the initial next time
                             interval

    if(rem(tInd,100) == 0)
        saveInd  = saveInd + 1;
        kWASEPsave(:,saveInd,:) = kWASEPprev;
    end
end

save("wasepN1000p500initFlat.mat","kTagged",
"kWASEPprev", "kWASEPsave")
```

For calculating the SOS from the WASEP

```
function [kSOS] = kWASEP2kSOS(kWASEP, kTagged)
  [m,k] = size(kWASEP)
  kSOS = zeros(m,k + 1);

  for i = 1:m %m simulations
      sos = zeros(1,m + 1);
      wasep = kWASEP(i,:);
      wasep = 2*wasep - ones(size(wasep));
      %put wasep in spin variables
```

```
        tagged = find(wasep,1); %impassable borders
        sos(tagged) = -tagged;
        for j = 1:tagged - 1
            sos(j) = -sum(wasep(j:tagged)) - tagged;
        end
        sos(tagged) = - tagged;
        for j = tagged + 1:k
            sos(j) = sum(wasep(tagged:j)) - tagged;
        end
        sos(k + 1) = sos(k - 1);
        kSOS(i,:) = sos;
    end
end
```

For linear and quadratic estimation

```
function [theta, res] = LeastSquares(x,y, degree)
   %takes pairs (x,y) and finds the line a + bx = y if
degree == 1
   %and the parabola ax^2 + bx + c if degree == 2
   %x, y must be a column vector and equal size
  [m,n] = size(x);
  if(m \langle n)
      x = x';
      y = y';
  end
  if degree == 1
  X = [ones(size(x)) x];
  else
  X = [ones(size(x)) x x.^2];
  end

  theta = (X'*X)\X'*y;
  res = sum((y - X*theta).^2);
end
```

B.2 Java

An animation to visualize the relation between the WASEP and the SOS. It is in the class wasepPanel that the simulations are made, the main class WASEPandSOS controls the animation.

```
import java.awt.*;
import java.awt.event.*;
import javax.swing.*;
import javax.swing.event.*;
import java.util.Random;
import java.util.PriorityQueue;
import java.util.Arrays;
import java.util.Collections;
import java.util.LinkedList;

class WasepPanel extends JPanel{
    double epsilon, tMax, currentTime;
    int initChoice; //which initial condition
    int xMax; //max nbr of positions + 1
    int[] xWASEP; // current configuration of WASEP
    Integer[] ySOS, ySOS2; // -''- SOS
    int tagged; //position of the tagged particle
    int first, nbr, initMin, timeIterations, initTagged;
                               //used in paintComponent()
    Random rand;
    PriorityQueue\langleJump> jumps; //potential jumps
                                        sorted by time
    int simTime;

public WasepPanel(){
  tMax = 30000.0; //generate Poisson process for tMax
                    long time
  timeIterations = 0;
  xMax = 101; // 100 positions, index [xMax - 1] is for
                  border conditions
  jumps = initializeJumps();
  initChoice = 0;
```

```
  xWASEP = initializeX();
  int i = 0;
  while(xWASEP[i] != 1){
     //xWASEP[i] == 1 for the first time is the tagged
particle
      i++;
  }
  tagged = i;

  ySOS = calculateY(xWASEP, tagged);
  initMin = Collections.min(Arrays.asList(ySOS));
  setBorder(BorderFactory.createLineBorder(Color.BLUE));
  nbr = xMax - 1;
  first = 0;
  epsilon = 0.25;
  rand = new Random();
      simTime = 60000;
    }

 public void step(long time ){
 //move one timestep = attempt to jump
   if(time \langle simTime){
      if(jumps.isEmpty()){
      jumps = initializeJumps();
      timeIterations++;
      }
   }

Jump j = jumps.poll();
int from = j.getNumber();
int to = from + j.getDirection();
double r;
currentTime = j.getTime();

if(from == xMax - 1){//new particle enters
    r = rand.nextDouble();
    if(j.getDirection() > 0){
    //positive direction = right jump to 0
```

```
      if(tagged == -1){
       tagged = 0;
       //the tagged particle re-enters the system
    }
   if(xWASEP[0] == -1 && r < 0.5){
   //position 0 empty,
   // and 50% probability of there being a particle
   // outside
       xWASEP[0] = 1;
       ySOS[0]-=2;
 }
  }else{//left to xMax-2
    if(xWASEP[xMax - 2] == -1 && r < 0.5){
        xWASEP[xMax - 2] = 1;
        ySOS[xMax - 1]+=2; //ySOS indices are
                           //"in between" xWASEP
    }
  }
}else if(from == 0 && j.getDirection() < 0){
//particle leaving from 0
    r = rand.nextDouble();
    if(xWASEP[0] == 1 && r < 0.5){//position 0 occupied
        // and 50% probability of there being a
        //particle outside
      if(tagged == 0){
         tagged = -1;
         //the tagged particle exits the system
      }
      xWASEP[0] = -1;
      ySOS[0]+=2;
    }
}else if(from == xMax - 2 && to > from) {
//particle leaving from xMax - 2
     r = rand.nextDouble();
     if(xWASEP[xMax - 2] == 1 && r \langle 0.5){
        xWASEP[xMax - 2] = -1;
        ySOS[xMax - 1]-=2;
      }
```

```
 }else{//particles move inside the system
     if(xWASEP[from] == 1 && xWASEP[to] == -1){
     if(tagged == from){
        tagged = to;
    }
    xWASEP[to] = 1;
    xWASEP[from] = -1;
    if(j.getDirection() \langle 0){
         ySOS[from]+=2;
    }else{
        ySOS[to]-=2;
    }
   }
  }
}

public int[] initializeX(){
    //sets the initial WASEP configuration from 3
choices of initial condition
        int[] temp = new int[xMax - 1];

switch (initChoice){
case 0:

for(int i = 0; i \langle 100; i++){//flat
    if(i%2 == 0){
temp[i] = -1;
    }else{
temp[i] = 1;
    }
}

return temp;
case 1:

for(int i = 0; i \langle 100; i++){// wedge
    if(i \langle 50){
temp[i] = -1;
```

```
    }else{
temp[i] = 1;
    }
}

return temp;
case 2:

for(int i = 0; i \langle 100; i++){//Brownian
    double r = rand.nextDouble();
    if(r > 0.5){
temp[i] = 1;
    }else{
temp[i] = -1;
    }
}

return temp;

}

return temp;
 }

public Integer[] calculateY(int[] x, int x0){
    //calculate SOS from WASEP
Integer[] ytemp = new Integer[xMax];
int x0_t; //the tagged particle
if(x0 > - 1){//tagged particle in visible part of system
    x0_t = x0;
}else{
    x0_t = 0;//if the tagged particle has left
     //the systemi t is set to be at
     //position 0 for these calculations
}

ytemp[0] = -sumBetween(x,0,x0_t) - x0_t;
```

```
for(int i = 0; i \langle x0_t; i++){
    ytemp[i+1] = -sumBetween(x, i + 1, x0_t) - x0_t;
}
ytemp[x0_t + 1] = -x0_t;
for(int i = x0_t + 1; i \langle xMax - 1; i++){
    ytemp[i + 1] = sumBetween(x, x0_t + 1, i) - x0_t;
}
return ytemp;
}

 public int sumBetween(int[] x, int a, int b){
    //sum of elements in x between index a and b
   int sum = 0;
   for(int i = a; i \langle b + 1; i++){
       sum+=x[i];
   }
   return sum;
}

public PriorityQueue\langleJump> initializeJumps(){
    //generates Poisson processes L and R for
    // all positions i
   Random rand = new Random();
   jumps = new PriorityQueue\langleJump>();
   Jump j;
   double tCurrent;//current time
   double q, p; //intensities;
   q = 1 + Math.sqrt(epsilon); //intensity left
   p = 1; //intensity right
   double n = p + q;
   q = q/n; //normalize
   p = p/n;
      for(int i = 0; i \langle xMax ; i++){
       tCurrent = 0;

    while(tCurrent \langle tMax){//left poisson process
    double u = rand.nextDouble(); //u ~ U(0,1)
```

```
    double x = -Math.log(1-u)/q; //x ~ Exp(1/q)
    tCurrent+=x;
    j = new Jump(i, tCurrent, -1);
    jumps.add(j);
    }
        tCurrent = 0;

    while(tCurrent \langle tMax ){//right poisson
                                  //process
        double u = rand.nextDouble(); //u ~ U(0,1)
    double x = -Math.log(1-u)/p; //x ~ Exp(1/p)
    tCurrent+=x;
    j = new Jump(i, tCurrent, 1);
    jumps.add(j);
    }

}
return jumps;
}

public void setInit(int c){
    //set initial condition choice in interface
initChoice = c;
    }

public void setFirst(int i){
    //set  leftmost particle shown
first = i;
    }

public void setZoom(int i){
    //set nbr of positions shown
nbr = 100 - i;
    }

public void updateEpsilon(int e){
    //set the value of epsilon and make new Poisson
processes
```

```
epsilon = (double) e/100;
jumps = initializeJumps();
    }

public void reset(){
    //reset to the initial configuration
jumps = initializeJumps();
xWASEP = initializeX();
        int i = 0;
while(xWASEP[i] != 1){
    i++;
}
tagged = i;
ySOS = calculateY(xWASEP,tagged);
ySOS2  = calculateY(xWASEP, tagged);
initMin = Collections.min(Arrays.asList(ySOS));
    }

public void paintComponent(Graphics gg){
    //makes graphics
Graphics2D g = (Graphics2D) gg;
super.paintComponent(g);
int height = this.getHeight();
int width = this.getWidth();
int x0axis = 7*height/10;
int stepSize = width/nbr;
int dotSize = stepSize - (stepSize/5);

g.setColor(Color.GRAY); //the grid the particles move in
g.drawLine(0,x0axis,width,x0axis);
g.drawLine(0,x0axis/2,width,x0axis/2);
for(int i = first; i \langle nbr + first; i++){
    g.fillOval(stepSize*(i - first), x0axis - 1, 2, 2);
}

g.setColor(Color.BLUE); //the particles
for(int i = first; i < Math.min(nbr+first, xMax - 1);
i++){
```

```
    if(tagged == i){
g.setColor(Color.GREEN); //the tagged particle in
different color
g.fillOval(stepSize*(i - first), x0axis - (dotSize )/2 ,
dotSize ,dotSize );
g.setColor(Color.BLUE);
    }else if(xWASEP[i] == 1){
g.fillOval(stepSize*(i - first), x0axis - dotSize/2,
dotSize,dotSize);
    }

}

g.setColor(Color.RED);//the linearly interpolated SOS
g.setStroke(new BasicStroke(dotSize/2 - 1));
for(int i = first; i \langle Math.min(nbr + first  ,
xMax - 1 ); i++){
    g.drawLine(stepSize*(i - first), x0axis +
initMin*stepSize - dotSize
        - stepSize*ySOS[i], stepSize*(i - first + 1),
x0axis + initMin*stepSize
        - dotSize - stepSize*ySOS[i + 1]);
}
}

public class WASEPandSOS extends JPanel{
    static JFrame frame;
    static JPanel mainPanel, buttonPanel, delayPanel,
epsilonPanel,
            initPanel, zoomPanel, zoomSlidePanel,
zoomFirstPanel;
    static JButton startButton, stopButton, resetButton;
    static JSlider delaySlider, epsilonSlider,
zoomSlider;
    static JLabel delayLabel, epsilonLabel, initLabel,
           zoomLabel1, zoomLabel2;
    static JComboBox initSOS;
    static JSpinner firstSpinner;
```

```
    static Timer timer;
    static WasepPanel wasepPanel;
    int maxDelay;
    static long startTime, simTime;

public WASEPandSOS(){
        //initializes the graphics components
        maxDelay = 2000; //max delay between graphics
updates in ms
        startTime = 0; //will be the time the start
button is pressed
simTime = 60000; //time the simulation will run in ms
timer = new Timer(10, new ActionListener(){
@Override
public void actionPerformed(ActionEvent e){
    long time = System.currentTimeMillis();
    wasepPanel.step(time - startTime);
    wasepPanel.repaint();
    if(time - startTime > simTime){
Timer t = (Timer) e.getSource();
t.stop();
    }


}
    });
timer.setRepeats(true);

frame = new JFrame("WASEP and SOS"); //main frame
        frame.setSize(514,514);
        frame.addWindowListener(new WindowAdapter(){
    public void windowClosing(WindowEvent windowEvent){
System.exit(0);
    }
});

wasepPanel = new WasepPanel(); //where the simulation is
run
```

```
    //add buttons to start, stop,  reset and set the
speed of the simulation
buttonPanel = new JPanel();
buttonPanel.setLayout(new FlowLayout());
startButton = new JButton("Start");
stopButton = new JButton("Stop");
resetButton = new JButton("Reset");
    startButton.addActionListener(new ActionListener(){
public void actionPerformed(ActionEvent e){
    timer.start();
    startTime = System.currentTimeMillis();
}
    });
stopButton.addActionListener(new ActionListener(){
public void actionPerformed(ActionEvent e){
    wasepPanel.printMovement();
    timer.stop();

}
    });
resetButton.addActionListener(new ActionListener(){
public void actionPerformed(ActionEvent e){
    wasepPanel.reset();
    wasepPanel.repaint();
}
    });

delayPanel = new JPanel(); //speed of simulation, or
time between updates
delayPanel.setLayout(new BoxLayout(delayPanel,
BoxLayout.Y_AXIS));
delaySlider = new JSlider(0,2000,1990);
delaySlider.addChangeListener(new ChangeListener(){
public void stateChanged(ChangeEvent e){
timer.setDelay(maxDelay - delaySlider.getValue());
System.out.println(maxDelay - delaySlider.getValue());
}
```

```
 });
delayLabel = new JLabel("Speed");
delayPanel.add(delaySlider);
delayPanel.add(delayLabel);

buttonPanel.add(startButton);
buttonPanel.add(stopButton);
buttonPanel.add(resetButton);
buttonPanel.add(delayPanel);

epsilonPanel = new JPanel(); //change value of asymmetry
epsilonPanel.setLayout(new BoxLayout(epsilonPanel,BoxLayout.Y_AXIS));
epsilonSlider = new JSlider(0,100,25);
epsilonLabel = new JLabel("Epsilon = " +
               (double) epsilonSlider.getValue()/100);
epsilonSlider.addChangeListener(new ChangeListener(){
public void stateChanged(ChangeEvent e){
    wasepPanel.updateEpsilon(epsilonSlider.getValue());
    epsilonLabel.setText("Epsilon = " +
                (double) epsilonSlider.getValue()/100);
   }
    });
epsilonPanel.add(epsilonSlider);
epsilonPanel.add(epsilonLabel);

initPanel = new JPanel(); //pick initial condition
initPanel.setLayout(new BoxLayout(initPanel,
BoxLayout.X_AXIS));
String[] initString = {"Flat", "Wedge", "Brownian"};
initSOS = new JComboBox(initString);
initSOS.setSelectedIndex(0);
    initSOS.addActionListener(new ActionListener(){
        public void actionPerformed(ActionEvent e){
        wasepPanel.setInit(initSOS.getSelectedIndex());
        wasepPanel.reset();
        wasepPanel.repaint();

    }
```

```
    });
    initPanel.add(initSOS);
initPanel.add(epsilonPanel);

zoomPanel = new JPanel();
//zoom is set by choosing the number of positions
displayed and
//which should be the leftmost position if the image
zoomSlider = new JSlider(0,90,0);

zoomLabel1 = new JLabel("zoom " );
firstSpinner = new JSpinner(new SpinnerNumberModel(0,0,100,20));
zoomLabel2 = new JLabel("lowest index");
firstSpinner.addChangeListener(new ChangeListener(){
public void stateChanged(ChangeEvent e){
 wasepPanel.setFirst((Integer) firstSpinner.getValue());
 wasepPanel.repaint();
}
  });
   zoomSlider.addChangeListener(new ChangeListener(){
public void stateChanged(ChangeEvent e){
  wasepPanel.setZoom(zoomSlider.getValue());
  zoomLabel1.setText("zoom " + (double) 100/(100 -
zoomSlider.getValue()) );
  wasepPanel.repaint();
    }
});
    zoomSlidePanel = new JPanel();
    zoomSlidePanel.setLayout(new
BoxLayout(zoomSlidePanel,
                             BoxLayout.Y_AXIS));
    zoomSlidePanel.add(zoomSlider);
    zoomSlidePanel.add(zoomLabel1);
    zoomFirstPanel = new JPanel();
    zoomFirstPanel.setLayout(new
BoxLayout(zoomFirstPanel,
                             BoxLayout.Y_AXIS));
    zoomPanel.setLayout(new BoxLayout(zoomPanel,
```

```
                        BoxLayout.Y_AXIS));
    zoomFirstPanel.add(firstSpinner);
    zoomFirstPanel.add(zoomLabel2);
    zoomPanel.add(zoomFirstPanel);
    zoomPanel.add(zoomSlidePanel);
    initPanel.add(zoomPanel);

mainPanel = new JPanel(new BorderLayout());
mainPanel.setBorder(BorderFactory.createLineBorder(Color.BLUE));
mainPanel.add(wasepPanel, BorderLayout.CENTER);
mainPanel.add(buttonPanel, BorderLayout.PAGE_END);
mainPanel.add(initPanel, BorderLayout.PAGE_START);

frame.add(mainPanel);
frame.setVisible(true);
}

public static void main(String[] args){
    SwingUtilities.invokeLater(new Runnable(){
    public void run(){
WASEPandSOS ws = new WASEPandSOS();
       }
   });
   }

}

}
class Jump implements Comparable<Jump>{
    private int number; //position where the particle
currently is
    private Double time; //time of jump
    private int direction; //1 if the jump is to the
right, -1 if left

    public Jump(int nbr, double t, int r){
   number = nbr;
   time = t;
```

```
   direction = r;
    }

public int  getDirection(){
return direction;
    }

public Double getTime(){
return time;
    }

public int getNumber(){
return number;
    }

public int compareTo(Jump j){ //sort by jump time
return this.time.compareTo(j.getTime());

    }

public void printout(){
System.out.println("from " + number + " in  direction "
+ direction +  " at time " + time);
    }
}
```

Master's Theses in Mathematical Sciences 2023:E77
ISSN 1404-6342

LUTFMA-3521-2023

Mathematics
Centre for Mathematical Sciences
Lund University
Box 118, SE-221 00 Lund, Sweden

http://www.maths.lu.se/